

1 **ADVANCING GLOBAL AEROSOL SIMULATIONS WITH SIZE-**
2 **SEGREGATED ANTHROPOGENIC PARTICLE NUMBER EMISSIONS**

3 FILIPPO XAUSA¹, PAULI PAASONEN^{1,5}, RISTO MAKKONEN¹, MIKHAIL
4 ARSHINOV², AIJUN DING³, HUGO DENIER VAN DER GON⁴, VELI-MATTI
5 KERMINEN¹, MARKKU KULMALA¹

6 ¹ *Division of Atmospheric Sciences, Department of Physics, University of*
7 *Helsinki.*

8 ² *Institute of Atmospheric Optics, SB RAS, 634055, Tomsk, Russia.*

9 ³ *Joint International Research Laboratory of Atmospheric and Earth System*
10 *Sciences, School of Atmospheric Sciences, Nanjing University, Nanjing*
11 *210023, China.*

12 ⁴ *TNO, Department of Climate, Air and Sustainability, Utrecht, the*
13 *Netherlands.*

14 ⁵ *International Institute for Applied Systems Analysis (IIASA), Laxenburg,*
15 *Austria*

16
17
18 Keywords: AEROSOL, NUMBER SIZE DISTRIBUTION, GAINS, GLOBAL CLIMATE
19 MODEL

20
21 ABSTRACT

22 Climate models are important tools that are used for generating climate
23 change projections, in which aerosol-climate interactions are one of the main
24 sources of uncertainties. In order to quantify aerosol-radiation and aerosol-
25 cloud interactions, detailed input of anthropogenic aerosol number emissions
26 is necessary. However, the anthropogenic aerosol number emissions are
27 usually converted from the corresponding mass emissions in precompiled
28 emission inventories through a very simplistic method depending uniquely
29 on chemical composition, particle size and density, which are defined for a
30 few very wide main source sectors. In this work, the anthropogenic particle
31 number emissions converted from the AeroCom mass in the ECHAM-HAM

32 climate model were replaced with the recently-formulated number emissions
33 from the Greenhouse Gas and Air Pollution Interactions and Synergies
34 (GAINS)-model. In the GAINS model the emission number size distributions
35 vary, for example, with respect to the fuel and technology. Special attention
36 was paid to accumulation mode particles (particle diameter $d_p > 100$ nm)
37 because of (i) their capability of acting as cloud condensation nuclei (CCN),
38 thus forming cloud droplets and affecting Earth's radiation budget, and (ii)
39 their dominant role in forming the coagulation sink and thus limiting the
40 concentration of sub-100 nanometers particles. In addition, the estimates of
41 anthropogenic CCN formation, and thus the forcing from aerosol-climate
42 interactions are expected to be affected. Analysis of global particle number
43 concentrations and size distributions reveal that GAINS implementation
44 increases CCN concentration compared with AeroCom, with regional
45 enhancement factors reaching values as high as 10. A comparison between
46 modeled and observed concentrations shows that the increase in number
47 concentration for accumulation mode particles agrees well with
48 measurements, but it leads to a consistent underestimation of both
49 nucleation mode and Aitken mode ($d_p < 100$ nm) particle number
50 concentrations. This suggests that revisions are needed in the new particle
51 formation and growth schemes currently applied in global modeling
52 frameworks.

53

54 1 Introduction

55 In recent years, the link between anthropogenic aerosol particles and climate
56 change has been a subject of several studies (e.g. Baker et al., 2015; Zhang
57 et al., 2016). Anthropogenic aerosol particles play an important role in the
58 global climate system via aerosol-radiation and aerosol-cloud interactions by
59 scattering and absorbing solar radiation and by acting as cloud condensation
60 or ice nuclei, thereby changing many cloud properties (Boucher et al., 2013).
61 The global and regional radiative effects of aerosol particles depend on the
62 spatial and temporal distribution of the aerosol number size distribution and
63 chemical composition (Lohmann and Feichter, 2005; Schulz et al., 2006;
64 Forster et al., 2007; Stier et al., 2007).

65 While anthropogenic primary emissions introduce cloud condensation nuclei
66 (CCN) directly into the atmosphere, a significant fraction of the global CCN
67 population is likely be formed through condensation of organic and other low-

68 volatility vapors onto ultra-fine particles (particle diameter $d_p < 100$ nm) in
69 the atmosphere (Spracklen et al., 2008; Merikanto et al., 2009; Kerminen et
70 al., 2012; Paasonen et al., 2013). Aerosol particles and their precursor vapors
71 are emitted from both biogenic and anthropogenic sources, in addition to
72 which they may also result from interactions between biogenic and
73 anthropogenic emissions (Spracklen et al., 2011; Shilling et al., 2013). The
74 increasing number concentration of accumulation mode particles decreases
75 the formation and growth of smaller particles by increasing the sink for
76 condensing vapor molecules, termed the condensation sink (CS, Kulmala et
77 al., 2001), and by increasing the coagulation sink for small freshly-formed
78 particles. Hence, the number concentration of accumulation mode particles
79 from primary emissions affects secondary aerosol formation. The effects of
80 these physical processes on future aerosol climate forcing requires
81 application of detailed aerosol microphysical schemes in global climate
82 models. Furthermore, the global uncertainty in CCN is highly sensitive to the
83 assumed emission size distribution (Lee et al., 2013).

84 The global aerosol climate model ECHAM-HAM (Stier et al., 2005; Zhang et
85 al., 2012) is a useful tool that aims at increasing our understanding of
86 aerosol-climate interactions. Past simulations performed with the ECHAM-
87 HAM include an extensive analysis of particle nucleation (Makkonen et al.,
88 2009; Kazil et al., 2010), aerosol properties (Roelofs et al., 2010), and
89 emission inventories implementation (Zhang et al., 2012). Although the
90 ECHAM-HAM has a detailed microphysics module for describing the aerosol
91 size distribution (Vignati et al., 2004), previous studies have not included an
92 exhaustive module for emitted particle number size distribution. Also in other
93 climate models, the mass-only aerosol input is a commonly applied setting
94 (Jones et al., 2007; Shindell et al., 2007). Advances in primary emission size-
95 distribution have been hindered by global climate model limitations in both
96 structure of the aerosol microphysics and the availability of size-segregated
97 emission inventories.

98 One of the emission inventories that has been widely used in ECHAM-HAM
99 simulations, as well as in other Earth System Models (Pozzoli et al., 2011;
100 Makkonen et al., 2009, 2012; Tonttila et al., 2015), is the Aerosol Inter
101 Comparison inventory, AeroCom (Dentener et al., 2006), developed for the
102 purpose of conducting improved simulations of aerosol-climate interactions
103 (Samset et al., 2014). However, the AeroCom emission inventory does not
104 include a specific framework for particle number emissions. Hence, the input

105 particle number emissions used in the simulations with AeroCom are
106 estimated from the particle mass emissions by the ECHAM-HAM during the
107 initialization routine. In more detail, the estimation of number emissions
108 consists of a simplistic multiplication of the given AeroCom mass emissions
109 by a mass-to-number conversion factor. Each conversion factor that is
110 applied for building the log-normal distribution is calculated by assuming
111 that the mass emissions for each main source sector are distributed to
112 predefined modes according to predefined densities, geometric mean radii
113 and standard deviations, as described by Vignati et al., (2004) and Stier et
114 al., (2005). This simplistic mass-to-number conversion factor does not
115 represent the relationship between the particle mass and number size
116 distributions in a realistic way, because such framework does not take into
117 account the variation of emitted particle number size distributions from
118 different emitting sources. The AeroCom inventory includes anthropogenic
119 activities, from which the mass-to-number converted emissions are split into
120 half between the Aitken and accumulation modes, and finally converted into
121 log-normal modes. However, the recently-developed inventories allow for
122 global aerosol simulations with a more detailed aerosol emission size
123 distribution (Paasonen et al., 2016) with the GAINS emission scenario model
124 (Greenhouse gas - Air pollution INteractions and Synergies; Cofala et al.,
125 2009; Amann et al., 2011). The GAINS inventory is organized into more
126 detailed anthropogenic sources than AeroCom, with different particle number
127 emissions and size distributions related to different fuels and technologies.

128 In this work, we first develop a novel module for anthropogenic particle
129 number emissions in Earth System Models. Our experiment, performed with
130 ECHAM-HAM, consists of replacing the mass-to-number converted
131 anthropogenic AeroCom aerosol emissions with number emissions from the
132 GAINS-model. In more detail, the implementation of the GAINS inventory is
133 performed by using ECHAM-HAM default assumptions for the AeroCom
134 inventory implementation. This study has a dual target: first, it aims at
135 improving the ECHAM-HAM capability for estimating particle number
136 concentrations, with a special focus on accumulation mode particles, and
137 second, it investigates the feasibility of using the GAINS model for global
138 climate modeling studies by running the ECHAM-HAM with both AeroCom and
139 GAINS inventories. We present a comparison between the novel GAINS
140 implementation and the default implementation of AeroCom in ECHAM-HAM,
141 including modeled particle number concentrations and size distributions, as
142 well as modeled CCN number concentrations. Finally, we compare the

143 modeled number size distributions with observations in different
144 environments around the world.

145

146 2 Materials and methods

147 2.1 The ECHAM5.5-HAM2 climate model

148 We used the global aerosol climate model ECHAM5.5-HAM2 (Stier et al.,
149 2005; Zhang et al., 2012) with the M7 microphysics module (Vignati et al.,
150 2004). The M7 describes the aerosol number size distribution with seven log-
151 normal modes, in which the Aitken, accumulation and coarse modes are
152 present in both the soluble and insoluble phases, while the nucleation mode
153 is present only as the soluble mode. The compounds modeled in our
154 simulations are black carbon (BC), organic carbon (OC), sulfate (SO₄), dust
155 and sea salt. The emission module used in ECHAM-HAM reads data for
156 anthropogenic, biogenic, wildfire, volcanic, agricultural emissions, secondary
157 organic aerosols (SOA) and shipping sources. In our experiments, we
158 modified only the part of the ECHAM-HAM source code that handles the
159 anthropogenic emissions. The model has a horizontal gaussian grid (192×96)
160 with a grid box size of ~200×200 km at the equator, and a vertical resolution
161 of 31 hybrid sigma layers.

162

163 2.1.1 Aerosol microphysics

164 The version of ECHAM-HAM used in this work includes nucleation,
165 condensation and coagulation modules. Previous studies have shown that
166 the implementation of an activation-type nucleation improves particle
167 number concentration estimations in modeling (Spracklen et al., 2010;
168 Makkonen et al., 2012). In our experiment, we coupled a binary sulphuric
169 acid-water nucleation scheme (Vehkamäki et al., 2002) with an activation-
170 nucleation scheme described by Paasonen et al., (2010, Eq. 10), in which the
171 nucleation rate (J) is a function of the activation coefficient and sulphuric acid
172 concentration, expressed as

$$173 \quad J = 1.7 \times 10^{-6} s^{-1} * [H_2SO_4] \quad . \quad (1)$$

174 The settings of our simulations included a specific module for SOA formation.
175 Here, we modeled the SOA formation with both kinetic condensation onto a
176 Fuchs-corrected surface area (CS) and partitioning according to a preexisting
177 organic mass (Riipinen et al., 2011; Jokinen et al., 2015). This SOA module
178 includes three biogenic volatile organic compound (BVOC) tracers: isoprene,
179 endocyclic monoterpenes and other monoterpenes, each having monthly
180 resolutions for emissions. We did not use any nucleation scheme for organic
181 vapors, because the simple activation-type nucleation, while not accurate for
182 individual sites, describes the nucleation in different environments
183 reasonably well (Paasonen et al., 2010). The particle growth from nucleation
184 size to the d_p of 3 nm was calculated according to Kerminen and Kulmala
185 (2002), considering both sulfuric acid and organic vapour condensation. More
186 details can be found in Makkonen et al. (2012).

187

188 2.1.2 Natural emissions

189 BVOC emissions were implemented using the MEGAN2 (Guenther et al.,
190 2006) model. MEGAN2 estimates biogenic emissions for about 150
191 compounds from different ecosystems, paying a particular attention to
192 monoterpenes. This framework takes into account several factors that
193 influence BVOC emissions, including the leaf age, soil moisture and light
194 environment. MEGAN2 was run offline and its output data were used for the
195 ECHAM-HAM input initialization.

196 All non-anthropogenic emissions, such as volcanic emissions, dimethyl-
197 sulfide (DMS, Kloster et al., 2006) emitted by the sea and dust, were taken
198 from AeroCom in both simulations. All emission data, excluding SOA
199 precursors, DMS emissions and wildfire, were input as annual-averages. As a
200 result, the seasonality in concentrations of anthropogenic compounds is
201 mostly due to the nudged meteorology.

202

203 2.1.3 Anthropogenic emissions

204 The first simulation was performed with the ECHAM-HAM default
205 implementation of anthropogenic emissions from the AeroCom inventory for
206 year 2000. The AeroCom emissions taken by the ECHAM-HAM are provided
207 by mass as $\text{kg m}^{-2} \text{s}^{-1}$ with a chemical differentiation that includes BC, OC and

208 SO₄, and a bi-level vertical distribution (2-zL) that consists of two surface
209 layers: a lower level below 100 meters above the sea level for emissions
210 from transportation and domestic combustion, and a higher level for
211 industrial activities whose emissions reach altitudes higher than 100 meters.
212 While BC does not require preprocessing during the simulation, input
213 emissions of OC and SO₄ undergo a further conversion during the
214 initialization routine: OC mass is converted into primary organic matter
215 (POM) mass with a multiplying factor 1.4 (Turpin et al., 2000; Kupiainen and
216 Klimont, 2007), and emissions containing sulfur (S) are input as both sulfur
217 dioxide (SO₂) and SO₄. The primary SO₄ particle fraction is estimated as 2.5%
218 of gaseous SO₂, as described by Dentener et al. (2006). The masses of BC
219 and POM are uniquely treated as Aitken mode particles ($d_p = 10-100$ nm).
220 The mass of SO₄ is divided between the Aitken mode, accumulation mode (d_p
221 = 100-1000 nm) and coarse mode ($d_p > 1$ μm) through a rough estimation:
222 the lower-surface-level SO₄ is split equally between the Aitken mode and
223 accumulation mode, whereas the higher-surface-level SO₄ is split equally
224 between the accumulation mode and coarse mode. The mass is then
225 converted by the model into a particle number size distribution. The mass-to-
226 number flux factors, expressed as $m2n$ in Figure 1, are embedded in the
227 emission-reading routine. The number of particles is calculated through the
228 generic function

$$229 \quad N = M/m \quad , \quad (2)$$

230 where M is the mass of given emissions and m is the average mass
231 estimated for a single particle. The particle mass m in Eq. (2) is extended in
232 the model according to the Hatch-Choate conversion equations (Hinds,
233 1982), in which the density, count median radius and standard deviation are
234 predefined for each chemical compound and size mode, as described by
235 Stier et al. (2005). The emission count median radius is fixed at 30 nm and
236 75 nm for the Aitken mode and accumulation mode, respectively, and the
237 standard deviation is set to 1.59 for all the modes except the coarse mode
238 for which it is 2.0. The species density is set to 1841 $kg\ m^{-3}$ for SO₄ (input in
239 the model as H₂SO₄) and 2000 $kg\ m^{-3}$ for BC and OC. Altogether, these
240 parameters differentiate the species according to their chemistry and
241 solubility. The number flux conversion is therefore expressed as

$$N = \frac{M}{\frac{4}{3} \cdot \pi \cdot \rho_i \cdot (\text{cmr}_{jk} \cdot \text{cmr2ram}_{jk})^3}, \quad (3)$$

244 where ρ is the density of a determined chemical compound i , and the
 245 expression in brackets is the mean radius of a particle with certain solubility j
 246 and size mode k . The quantity cmr is the predefined count median radius as
 247 it is expressed in the model code, while cmr2ram is a conversion factor that
 248 multiplies cmr in order to estimate the radius of average mass. The cmr2ram
 249 factor depends uniquely on the standard deviation of the log-normal particle
 250 number distribution.

251

252 2.2 Emission scenario model GAINS

253 The GAINS (Greenhouse gas - Air pollution Interactions and Synergies) model
 254 is an integrated assessment model developed at IIASA (International Institute
 255 for Applied Systems Analysis) in Laxenburg, Austria (Amann et al, 2011). In
 256 order to calculate the emissions related to specific anthropogenic source
 257 sectors, it combines the information of the annual level of the anthropogenic
 258 activities, amounts of different fuels consumed for combustion activities,
 259 shares of different emission abatement technologies, and emission factors
 260 for different activity-fuel-technology-combinations.

261 The GAINS scenarios include information on the annual activity levels and
 262 shares of emission control technologies for nearly 170 regions, being
 263 countries or parts or groups of countries, in five-year intervals from 1990 to
 264 2050. The activity levels are based on national and international statistics,
 265 latter available from International Energy Agency (IEA), Organisation for
 266 Economic Co-operation and Development (OECD), United Nations (UN) and
 267 Food and Agriculture Organization of the United Nations (FAO) and Eurostat,
 268 and the shares of control technologies are derived from national and
 269 international information on the related legislation, discussion with national
 270 experts and scientific publications. The emission factors for all combinations
 271 of source sectors, fuels and technologies are determined from the scientific
 272 publications or measurement databases. For detailed description of sources
 273 and methods to derive underlying particulate matter emissions see Klimont
 274 et al. (2016).

275 The particle number emission factors with the related number size
276 distributions were recently implemented to GAINS (Paasonen et al., 2016).
277 This implementation allowed for detailed assessment of particle number
278 emissions with more than 1000 measures controlling emissions in each of
279 the close to 170 regions, and in internally consistent manner with emissions
280 of other air pollutants and greenhouse gases. The GAINS particle number
281 emissions are known to be subject to uncertainties, especially in terms of
282 nucleation mode emissions, but the major particle number sources, such as
283 road transport and residential combustion, are reasonably well represented
284 down to the control technology level. The determination of emission factors
285 for particle number emissions and particle size distributions is based on the
286 European particle number emission inventory developed by TNO (Denier van
287 der Gon et al., 2009, 2010).

288 In this study, we applied the gridded particle number emissions for year
289 2010 (Paasonen et al., 2016), in which the activity measures and emission
290 abatement technology shares are based on the 'ECLIPSE version 5' inventory
291 (Klimont et al., 2016) developed within the EU FP7 ECLIPSE project (Stohl et
292 al., 2015). The gridded data and their brief characterization is freely
293 available from the IIASA website:

294 <http://www.iiasa.ac.at/web/home/research/researchPrograms/air/PN.html>.

295

296 2.3 GAINS implementation in M7

297 In the second simulation, the sub-module that converts the input mass to the
298 number flux described in Eqs. (2-3) was switched off and we implemented
299 the recently-developed 2010 GAINS anthropogenic emissions (Paasonen et
300 al., 2016; see also section 2.1.2). The emission sectors considered for our
301 experiment included the energy production, flares, industrial combustion and
302 processes, transportation, waste combustion and domestic/commercial
303 combustion. A detailed description of the sectors and emission factors is
304 presented in Paasonen et al. (2016).

305 The number size distribution inventory provided by GAINS is organized into
306 nine size bins with a geometric diameter ranging from 3 nm to 1000 nm.
307 However, in this study we implemented the GAINS inventory for the Aitken
308 mode and accumulation mode only ($d_p = 10-1000$ nm), so that the particle
309 number implementation was consistent with the AeroCom simulation which

310 lacked the nucleation mode conversion factor in the source code aerosol
311 module. The conversion of GAINS emissions from sectional to modal size
312 distribution was performed by splitting the total particle number
313 concentration from the GAINS inventory between the Aitken and
314 accumulation modes using the GAINS sectional particle diameter of 100 nm
315 as the limit between these two modes. The rest of the modal parameters, i.e.
316 the modal median radii and standard deviations, were taken as the default
317 values of the ECHAM-HAM modal properties (Stier et al., 2005). This choice of
318 implementation does not fully exploit all the information available in the
319 GAINS size distribution, because the default ECHAM-HAM emission module
320 does not allow the emission diameter to vary on a per-gridbox basis.
321 Although it would be possible to upgrade the ECHAM-HAM in this sense, it
322 would be quite laborious and beyond the scope of our study. It should be
323 noted that the ratio of Aitken to accumulation mode emissions can vary
324 between grid cells in both AeroCom and GAINS. In AeroCom this variation is
325 due to different mass-to-number conversion factors for different emission
326 sectors, but in GAINS the size distributions are different also for different
327 technologies and fuels within the emission sectors (e.g. different vehicle
328 technologies, different domestic stove categories, diesel fuels with different
329 sulfur contents, different coal types).

330 In the GAINS simulation we kept the AeroCom gas phase sulfur and coarse
331 SO₄ in order to identify the global impact of GAINS implementation on
332 submicron particles. Furthermore, we used the same bi-level 2-zL scheme as
333 for the SO₄ vertical distribution in AeroCom: emissions from the
334 transportation, agriculture fires, waste combustion and domestic combustion
335 were put into the lower level (<100 m a.s.l.), whereas the energy, flares,
336 industry and power plant sectors of GAINS were implemented into the higher
337 level (>100 m a.s.l.).

338 GAINS provides the number emissions without chemical speciation and
339 vertical distribution (see Table 1), and separately mass emissions of particle
340 mass, particulate OC and BC, as well as gaseous pollutants, including SO₂.
341 However, distributing the different compounds between the different number
342 sizes bins is non-trivial task which requires, in order to be properly
343 completed, elaboration of the proper GAINS model, not only the
344 implementation. For this reason, we decided to use the default ECHAM-HAM
345 particle composition from AeroCom in this study and leave the
346 implementation of GAINS chemical composition for future studies. We

347 followed a series of steps in order to partition the GAINS raw data into BC,
348 POM and SO₄ in a consistent format for the model. Table 1 and Figure 1
349 visually illustrate the implementation framework. In more detail, we (I) off-
350 line converted AeroCom mass into number using ECHAM-HAM factors, (II)
351 estimated the chemical species fraction among the respective Aitken mode
352 and accumulation mode in AeroCom numbers, (III) applied such fractions to
353 the total Aitken mode and accumulation mode particle numbers in the GAINS
354 to have the correspondent BC, OC and SO₄ repartition, and finally, IV) used
355 the mass-to-number factors used in (I) to estimate the speciated GAINS
356 mass. The above framework highlights that, while the mass-to-number
357 conversion factors are unaltered for each specific mode, the mass taken from
358 AeroCom and GAINS inventories by the ECHAM-HAM is different. Although
359 the mass is not the focus of our study, this difference may have further
360 implications in terms of simulating particle mass concentrations (see the
361 supplementary material for the total PM_{2.5} concentrations).

362 Shipping emissions are embedded in the AeroCom inventory, but not
363 included in GAINS. In our experiment, we masked out the AeroCom shipping
364 emissions with a land-sea mask produced by applying Climate Data Operator
365 (CDO) to the AeroCom. Hence, shipping emissions were not taken into
366 consideration. Biomass burning emissions are included as mass-based
367 emissions from the AeroCom inventory.

368

369 2.4 Simulation setup

370 Our experiment consisted of two one-year simulations, using identical model
371 settings but different inventories for anthropogenic sources: AeroCom and
372 GAINS (see Sect. 2.3). The experiment run was set to start indicatively on
373 October 1, 2009 and end on December 31, 2010 with a three-month spin-up
374 period and one-hour time resolution for the output. The modeled data for our
375 analysis were collected from January 1, 2010 to December 31, 2010. The
376 model was nudged against 2010 ECMWF ERA-Interim (Berrisford et al., 2011)
377 observed meteorology in order to reduce noise in model estimations and to
378 increase the statistical significance of the eventual anthropogenic aerosol
379 perturbation signal (Kooperman et al., 2012).

380

381 2.5 Comparison with observation

382 Our study focused on particle number concentration and size distributions
383 along with CCN concentrations at the supersaturations of 0.2% (CCN0.2) and
384 1.0% (CCN1.0). We compared the modeled particle number concentrations
385 and size distributions against observations collected from 11 sites around the
386 world. A detailed description of the observation data is illustrated in Table 2.
387 The modeled data extracted from all sites were averaged over the year and
388 plotted against observations to investigate the overall model performance. In
389 addition to the visual comparison between the modeled and observed
390 concentrations, we calculated the relative bias, i.e. the ratio of modeled and
391 measured concentrations, for each measurement site. For the sites where
392 the ratio was smaller than one, the bias was replaced with its multiplicative
393 inverse. By this way we were able to calculate and compare the averages of
394 the relative biases at different sites between the model runs.

395 The particle number concentration and mean particle radius of the whole
396 output data were used for plotting the number distributions from 6 of the 11
397 original sites, which were chosen to represent areas with a strong presence
398 of anthropogenic emissions (Nanjing, Sao Paulo and Tomsk) as well as areas
399 dominated by biogenic emissions (Hyytiälä, K-Pusztta and Värriö). In both
400 annual-average and number distribution comparisons, the modeled layer
401 closest to Earth's surface was chosen for analysis. Modeled CCN
402 concentrations were studied by comparing simulations with AeroCom
403 emissions against those from GAINS emissions for both CCN0.2 and CCN1.0.
404 CCN concentrations were extracted and averaged from the lowest three
405 model layers in order to reduce background noise in mapping the global
406 concentrations. Due to the coarse grid size and inhomogeneous sources
407 around measurement sites, the evaluation against observations is not
408 expected to yield one-to-one validation of aerosol concentrations (Schutgens
409 et al., 2016).

410

411 3 Results and discussion

412 Here we show the comparison between AeroCom and GAINS implementation
413 before (emissions, section 3.1) and after (atmospheric concentrations,
414 sections 3.2 and 3.3) running the ECHAM-HAM model. Our experiment was
415 performed with the same model settings in both simulations and it was
416 nudged against meteorology data. As a result, our analysis focused merely
417 on the differences between the particle number emissions of the two

418 inventories and their different effects on modeled particle concentrations. In
419 the following sections, we will first show the difference between AeroCom
420 and GAINS in terms of input emissions, after which we will compare the
421 model-simulated particle number concentrations and size distributions with
422 observational data. Finally, we will assess the effect of the GAINS
423 implementation on global CCN concentrations.

424

425 3.1 Differences in particle number emissions

426 In this section, we present a preliminary assessment of input emissions to
427 illustrate the main differences between the two inventories before starting
428 the simulation. Table 3 shows global anthropogenic emissions and their ratios
429 between GAINS and AeroCom for the whole domain. When the emissions
430 were globally averaged (R_{tot}), GAINS showed higher total number emissions
431 by a factor of 2.2. However, when looking at individual grid cells, the total
432 particle number emission ratios between AeroCom and GAINS had a large
433 spatial variability (Figure 2), even though the median value of this ratio was
434 very close to one (see R_{grid} in Table 3). Figure 3 shows the spatial distribution
435 of both emissions inventories. Globally, the Aitken to accumulation mode
436 particle emission ratio was about two orders of magnitude in AeroCom
437 emissions, while being less than a factor four in GAINS emission. The
438 averaged emission ratios demonstrate that accumulation mode emissions
439 play a critical role in the GAINS implementation, with both R_{tot} and R_{grid} ratios
440 increasing dramatically compared with AeroCom. The averaged Aitken mode
441 particle emissions from GAINS did not show a similar increase, and the R_{grid}
442 median value was even lower than that in the AeroCom emissions. The R_{tot}
443 and R_{grid} ratios of Aitken mode emissions were 1.7 and 0.7, respectively. This
444 difference shows that the Aitken mode particle emissions are quantitatively
445 higher in GAINS than in AeroCom when their geographical distribution
446 differences are not taken into account. However, when the inventories were
447 compared by confronting each grid cell one by one, AeroCom emissions were
448 higher than GAINS emissions in a prevalent area of the global domain.

449 In the ECHAM-HAM, fossil fuel and biofuel are emitted into the Aitken
450 insoluble mode, and are converted into soluble particles after sulfate
451 condensation. In GAINS, the particles estimated to contain BC are distributed
452 into particle size bins at around 100 nm (Paasonen et al., 2016). The

453 difference between the diameters of emissions from fossil fuel and biofuel
454 combustion is the major reason behind the differences in accumulation mode
455 emissions and concentrations.

456 The differences in Aitken and accumulation mode emissions between GAINS
457 and AeroCom implementations originate from three main differences. Firstly,
458 the GAINS emission factors, especially in traffic and residential combustion
459 sectors, are directly based on literature or databases of particle number
460 emissions, whereas in AeroCom the number emissions are converted from
461 mass emissions. This causes differences in the relative shares of different
462 source sectors in the emission size distributions. Secondly, the original
463 emission size distributions in GAINS contains from one to three different
464 modes, whereas in AeroCom the emissions are represented with only one
465 mode. In many GAINS sources, e.g. road transport, the mode with a larger
466 mean emission diameter contributes significantly to the emission of particles
467 with $d_p > 100$ nm, even though the total number emission is clearly
468 dominated by a mode with a smaller mean diameter. Finally, as stated
469 earlier, the GAINS emission size distributions are different for different
470 technologies and fuels, in diesel powered road transport also for different
471 fuel sulfur contents. This increases the regional variability of the emissions.

472

473 3.2 Simulated particle number concentrations and size distributions

474 Here we present the core of our analysis, which includes an assessment of
475 the modeled particle number concentrations against observations. Figure 4
476 shows the annual-averaged modeled particle concentration in comparison
477 with observations from eleven sites. Overall, both emission inventories
478 showed a tendency to underestimate particle number concentrations in
479 model simulations, especially for the locations with high observed particle
480 number concentrations. The underestimation of the highest particle
481 concentrations might be, at least partly, related to the spatial resolution of
482 ECHAM-HAM, due to which the typically high particle concentrations near
483 urban or industrial areas will be distributed evenly into a large model grid
484 cell (Stier et al., 2005). A comparison of the model results with the
485 observational data shows that the GAINS implementation significantly
486 improved the reproduction of observed concentrations in accumulation mode
487 ($d_p > 100$ nm), being closer to observations than AeroCom at all 11 sites. For
488 the Aitken mode ($d_p = 10-100$ nm), similar improvement was not reached, as

489 the observed concentrations were better reproduced with AeroCom than with
490 GAINS at 8 sites. The average relative bias described in section 2.5 for the
491 accumulation mode concentrations with GAINS emissions was 2.37 and with
492 AeroCom emissions 3.51. The average relative bias for the Aitken mode
493 concentrations were 2.25 and 2.12 with GAINS and AeroCom emissions,
494 respectively. It should be noted that the emissions from different emission
495 sources and observations are not all from the same years. However, even
496 though the GAINS emissions are for year 2010 and AeroCom emissions for
497 year 2000 (and observations for the years indicated in Table 2), the
498 differences in the modeled concentrations with GAINS and AeroCom at most
499 polluted sites, reaching factors of 2 and above, cannot be expected to
500 originate from differences in emissions between 2000 and 2010.

501 Figure 5 shows the modeled particle number size distributions against
502 observations at 6 measurement sites. The size distributions modeled with
503 the GAINS emissions agreed relatively well with the measurements for the
504 accumulation mode, whereas the nucleation and Aitken modes were
505 underestimated in simulations with both emission inventories. GAINS
506 underestimated the Aitken mode particle concentrations more heavily than
507 AeroCom, by a factor of two to three in Hyytiälä, Värriö and Kpuszta,
508 suggesting that the higher CS associated with higher accumulation mode
509 particle emissions in GAINS had a significant impact on modeled ultra-fine
510 particle number concentrations. In addition, Hyytiälä and Värriö are regions
511 in which BVOC emissions and clean air are the key influencing factors for
512 new particle formation and particle growth (Ruuskanen et al., 2007; Corrigan
513 et al., 2013; Liao et al., 2014). This was reflected in the model results:
514 particle number size distributions in Hyytiälä and Värriö were quite similar
515 between the two simulations based on different anthropogenic emission
516 inventories. Contrary to this, Nanjing, Sao Paulo and Tomsik are areas with
517 strong influences by anthropogenic emissions, so that in comparison with
518 AeroCom, the simulations with GAINS emissions produced higher
519 accumulation mode and Aitken mode particle number concentrations as well
520 as better agreements with the observations in these regions. Nevertheless,
521 the model was not able to reach the observed ultra-fine particle
522 concentration in either simulation in most areas, and the higher CS in GAINS
523 significantly reduced particle number concentrations of the smallest particles
524 in most regions. Some areas showed a dramatic reduction in simulated ultra-
525 fine particle number concentrations e.g. in Nanjing the whole modeled
526 nucleation mode was wiped out when using the GAINS emissions.

527 The above results suggest that in the ECHAM-HAM the current nucleation and
528 growth schemes may need further revisions. However, it is also likely that
529 the anthropogenic emissions of especially nucleation mode particles in
530 GAINS are still severely underestimated for many source sectors (Paasonen
531 et al., 2016). This is because many of the measurements, on which the
532 GAINS emission factors are based, are not sensitive to non-solid nucleation
533 mode particles, such as those formed via nucleation of sulfur or organic
534 vapors immediately after the combustion or at small downwind distances in
535 plumes from different combustion sources (Stevens and Pierce, 2013). It
536 should also be noted that our study does not include any sensitivity analysis
537 based on the primary sulfate emissions parameterization (Luo and Yu, 2011).
538 In addition, the lower modeled Aitken mode particle concentrations from
539 GAINS emissions may, in some parts of the global domain, be also related to
540 possible overestimations in the accumulation mode particle emissions in the
541 GAINS model, which are consequently affecting the formation and growth of
542 smaller particles. Nonetheless, all the model versus observation comparisons
543 between the simulations clearly represent a consistent challenge for climate
544 models in modeling ultra-fine particle number size distributions.

545 Figure 6 shows absolute annual-average particle concentrations for the
546 accumulation mode and Aitken mode with both AeroCom and GAINS
547 emissions. While the regional distributions had similar patterns in both
548 simulations, there were evident differences when looking at the two size
549 modes. Accumulation mode particle concentrations were higher for the
550 simulation with the GAINS emission in most regions, which is consistent with
551 the input emissions assessment. The differences were particularly evident
552 over the developing areas where anthropogenic activities represent the main
553 source of atmospheric particles, especially in South America, central Africa,
554 India, China and south-east Asia. As observed in Figure 5, the high
555 accumulation mode particle number concentrations in the simulation with
556 the GAINS emission has a critical effect on Aitken mode particle
557 concentrations at most sites. A peculiar pattern is observed in China where
558 the dominant presence of anthropogenic sources from GAINS led the model
559 to predict high concentrations of ultra-fine particles. The decrease in GAINS-
560 derived Aitken mode particle number concentrations in areas where
561 emissions were actually higher than the AeroCom emission implies that
562 Aitken mode particles had been removed, or their secondary production was
563 hindered, by the prominent increase of the CS caused by a higher number of
564 emitted accumulation mode particles. It's important to note that while the

565 accumulation mode particle concentration played a major role in increasing
566 the CS (hence boosting the Aitken mode particles removal), the difference in
567 the particle number concentrations of the Aitken mode might be also due to
568 the lower Aitken mode emissions in GAINS (see Table 3). However, in this
569 research it was not possible to quantify how much of this difference was
570 actually due to the different Aitken mode particle number emissions.

571

572 3.3 Concentrations and sources of CCN

573 This section presents the impact of particle emissions on atmospheric CCN
574 concentrations on annual and seasonal perspectives. It is important to note
575 that the applied anthropogenic number emissions did not have a seasonal
576 variation, so the seasonal differences are entirely due to the variation of
577 other emissions, and mainly to the strong temperature dependence of
578 biogenic SOA formation affecting the CCN concentration (Paasonen et al.,
579 2013). Our results showed clear differences in the simulated CCN
580 concentrations between the two primary emission inventories, and these
581 differences depended strongly on the considered supersaturation (Table 4,
582 Figure 7 and 8).

583 At the 0.2% supersaturation, the CCN concentrations were higher with the
584 GAINS emissions compared with the AeroCom emissions in practically all the
585 regions and during all seasons (Figure 8). The annual-average CCN_{0.2}
586 concentration ratio between the GAINS and AeroCom was two to three in
587 most areas, with peaks of four to ten in south America, central Africa and
588 east Asia (Figure 7). However, relatively high accumulation mode particle
589 concentrations were observed in India, China and south-east Asia (see Figure
590 6), and also an increase in absolute CCN_{0.2} concentration due to
591 anthropogenic emissions was observed in eastern China and south-east Asia.
592 Our analysis of the seasonality revealed that the difference between GAINS
593 and AeroCom simulations in terms of CCN_{0.2} concentrations was the largest
594 during the cold season in January, with boreal and arctic regions showing an
595 increment of GAINS/AeroCom CCN_{0.2} ratio up to a factor of seven to ten. The
596 southern hemisphere also displayed notable differences in both South
597 America and South-East Asia, with GAINS/AeroCom CCN_{0.2} ratios of three to
598 ten during the warmest season.

599 At the supersaturation of 1.0%, a significant fraction of Aitken mode particles
600 is capable of acting as CCN. Opposite to the CCN0.2 concentrations, the
601 simulated CCN1.0 concentrations with the GAINS emissions were lower than
602 with AeroCom emissions, with a GAINS/AeroCom ratio between 0.5 and 1 in
603 most regions (Figure 7). Our seasonality analysis showed that the simulation
604 with the GAINS inventory produced higher CCN1.0 concentrations than
605 AeroCom in Europe, India and East Asia during the winter. However, such
606 ratio was equal to one or below in most regions, except eastern Asia, during
607 the warmer seasons. The substantially lower CCN1.0 concentrations with
608 GAINS emissions arise from the relatively similar Aitken mode number
609 emissions between GAINS and AeroCom, but significantly larger CS from
610 GAINS, causing a decrease in secondary ultrafine particle formation.
611 However, in China and South-East Asia, the annual CCN1.0 concentration
612 from GAINS was higher than from AeroCom by at least a factor of two,
613 suggesting that these regions may play a key role in contributing for the
614 global anthropogenic emissions and increment of CCN.

615 It is important to remark that the substantial differences in CCN
616 concentrations illustrated above are linked to the implementation of different
617 inventories, and therefore the modeled estimations might be affected by
618 uncertainties of the GAINS model as well. Furthermore, it may be questioned
619 whether the ECHAM-HAM is actually able to estimate CCN concentrations
620 with GAINS better than with AeroCom. This goes beyond the fundamental
621 goal of this study, which is to address the feasibility of using GAINS
622 emissions in global climate modeling. However, the modeled GAINS
623 accumulation mode particle number concentrations agree with observation
624 significantly better than AeroCom. This, based on the sensitivity analysis by
625 Lee et al. (2013), suggests that the GAINS implementation is likely to
626 estimate CCN concentrations better than AeroCom. In any case, further
627 studies are needed to address the contribution of the GAINS model in
628 improving modeled CCN concentration. Furthermore, it would be beneficial to
629 investigate how the applied nucleation scheme, combined with the GAINS
630 anthropogenic emissions, affects the estimation of CCN concentration to
631 better identify the driving forces behind the uncertainties of modeling
632 particle number size distributions with the global climate models.

633

634 4 Conclusions

635 The outcome of our experiment shows that the most significant differences
636 between the GAINS and AeroCom emissions inventories are (i) the particle
637 number emissions in the Aitken mode and accumulation mode, and (ii) the
638 geographical distribution of the particle number emissions over the global
639 domain. The accumulation mode particle emissions from GAINS are
640 significantly higher than AeroCom, by factors from 10 to 1000, thus
641 potentially resulting in dramatic increases in climatically active primary
642 particles and simultaneous decreases in secondary ultrafine particle
643 formation due to higher values of CS and coagulation sink.

644 In comparison to AeroCom emissions, GAINS emissions produced much
645 higher accumulation mode particle concentrations, but the consequently
646 higher CS and coagulation sink led to lower Aitken mode concentrations with
647 GAINS emissions than with AeroCom emissions. In comparison to observation
648 data at eleven measurement sites, the modeled annual-averaged
649 concentrations with GAINS emissions performed better than with AeroCom
650 emissions, in terms of bringing the modeled accumulation mode particle
651 concentrations closer to observation at all eleven sites, and Aitken mode
652 particle concentrations closer to observation at three sites. However, a
653 higher underestimation was observed in the simulation with GAINS emissions
654 for particles with $d_p < 30$ nm.

655 The underestimation of $d_p < 30$ nm particle concentrations in the simulation
656 with GAINS emissions highlighted the sensitivity of nucleation mode and
657 Aitken mode particle concentrations to CS and coagulation sink. This
658 underestimation is presumably partly caused by underestimations in
659 emissions of non-solid nucleation/Aitken mode particles in the GAINS model
660 (Paasonen et al., 2016). As a next step, the modules for nucleation and
661 subsequent growth and the sensitivity of the concentrations of sulfuric acid
662 (the main precursor in the applied nucleation parameterization) to altered CS
663 should be revisited.

664 It is important to note that the simulations performed in this study did not
665 implement an up-to-date secondary organic aerosols (ELVOCS) nucleation
666 scheme, nor a seasonal cycle of anthropogenic emissions, which may
667 represent a further step to reduce the gap between the modeled and
668 observed concentrations. Finally, given the high spatial variability of global
669 emissions, more observation data and the establishment of new

670 measurement stations in varying environments are urgently needed to better
671 evaluate the model results.

672

673 Acknowledgements

674 This project was funded by the MAJ JA TOR NESSLING grant n. 201600369
675 and the Academy of Finland Center of Excellence (FCoE) grant n. 307331.

676 Particle number size distributions at Melpitz were provided by Wolfram
677 Birmili, Kay Weinhold, André Sonntag, Birgit Wehner, Thomas Tuch, and
678 Alfred Wiedensohler (Leibniz Institute for Tropospheric Research, Leipzig,
679 Germany).

680 Particle number size distributions at Hohenpeissenberg were provided by
681 Harald Flentje and Björn Briel (German Weather Service, Hohenpeissenberg,
682 Germany). Both measurements were supported by the German Federal
683 Environment Ministry (BMU) grant UFOPLAN 370343200, project duration
684 2008-2010. Both data sets can be publicly accessed through the German
685 Ultrafine Aerosol Network (GUAN) at <https://doi.org/10.5072/guan>.

686 Particle number size distributions at Botsalano were provided by Ville Vakkari
687 and Lauri Laakso (Finnish Meteorological Institute, Helsinki, Finland).

688 Particle number size distributions at Sao Paulo were provided by John
689 Backman (Finnish Meteorological Institute, Helsinki, Finland).

690 Particle number size distributions at San Pietro Capofiume (Po Valley) were
691 provided by Ari Laaksonen (Finnish Meteorological Institute, Helsinki,
692 Finland).

693 We thank Chris Heyes and Zbigniew Klimont from the Air Quality and
694 Greenhouse Gases program at IIASA, and Kaarle Kupiainen from IIASA and
695 Finnish Environment Institute (SYKE) for their help and communication.

696 The EU FP7 BACCHUS project (grant n. 603445) and the Nordic Center of Excellence
697 eSTICC (Nordforsk grant n. 57001) are acknowledged for financial support.

698

699

- 701 Amann, M., Bertok, I., Borcken-Kleefeld, J., Cofala, J., Heyes, C., Höglund-Isaksson, L., Klimont,
702 Z., Nguyen, B., Posch, M., Rafaj, P., Sandler, R., Schöpp, W., Wagner, F. and Winiwarter, W.:
703 Cost-effective control of air quality and greenhouse gases in Europe: Modeling and policy
704 applications, *Environ. Model. Softw.*, 26(2), 1489–1501, 2011.
705
- 706 Backman, J., Rizzo, L. V., Hakala, J., Nieminen, T., Manninen, H. E., Morais, F., Aalto, P. P.,
707 Siivola, E., Carbone, S., Hillamo, R., Artaxo, P., Virkkula, A., Petäjä, T., and Kulmala, M.: On the
708 diurnal cycle of urban aerosols, black carbon and the occurrence of new particle formation
709 events in springtime São Paulo, Brazil, *Atmos. Chem. Phys.*, 12, 11733–11751,
710 doi:10.5194/acp-12-11733-2012, 2012.
711
- 712 Baker, L. H., Collins, W. J., Olivie, D. J. L., Cherian, R., Hodnebrog, Ø., Myhre, G., and Quaas,
713 J.: Climate responses to anthropogenic emissions of short-lived climate pollutants, *Atmos.*
714 *Chem. Phys.*, 15, 8201–8216, doi:10.5194/acp-15-8201-2015, 2015.
715
- 716 Berrisford, P., Kållberg, P., Kobayashi, S., Dee, D., Uppala, S., Simmons, A. J., Poli, P. and Sato,
717 H.: Atmospheric conservation properties in ERA-Interim. *Quarterly Journal of the Royal*
718 *Meteorological Society* 137:1381–1399, 2011.
719
- 720 Birmili, W., Weinhold, K., Rasch, F., Sonntag, A., Sun, J., Merkel, M., Wiedensohler, A., Bastian,
721 S., Schladitz, A., Löschau, G., Cyrys, J., Pitz, M., Gu, J., Kusch, T., Flentje, H., Quass, U.,
722 Kaminski, H., Kuhlbusch, T. A. J., Meinhardt, F., Schwerin, A., Bath, O., Ries, L., Gerwig, H.,
723 Wirtz, K., and Fiebig, M.: Long-term observations of tropospheric particle number size
724 distributions and equivalent black carbon mass concentrations in the German Ultrafine
725 Aerosol Network (GUAN), *Earth Syst. Sci. Data*, 8, 355–382, doi:10.5194/essd-8-355-2016,
726 2016.
727
- 728 Boucher, O., Randall, D., Artaxo, P., Bretherton, C., Feingold, G., Forster, P., Kerminen, V.-M.,
729 Kondo, Y., Liao, H., Lohmann, U., Rasch, P., Satheesh, S.K., Sherwood, S., Stevens, B. and
730 Zhang, X.Y.: Clouds and aerosols. In *Climate Change 2013: The Physical Science Basis.*
731 *Contribution of Working Group I to the Fifth Assessment Report of the Intergovernmental*
732 *Panel on Climate Change.* T.F. Stocker, D. Qin, G.-K. Plattner, M. Tignor, S.K. Allen, J.
733 Doschung, A. Nauels, Y. Xia, V. Bex, and P.M. Midgley, Eds. Cambridge University Press, 571–
734 657, doi:10.1017/CBO9781107415324.016, 2013.
735
- 736 Corrigan, A. L., Russell, L. M., Takahama, S., Äijälä, M., Ehn, M., Junninen, H., Rinne, J., Petäjä,
737 T., Kulmala, M., Vogel, A. L., Hoffmann, T., Ebben, C. J., Geiger, F. M., Chhabra, P., Seinfeld, J.
738 H., Worsnop, D. R., Song, W., Auld, J., and Williams, J.: Biogenic and biomass burning organic
739 aerosol in a boreal forest at Hyytiälä, Finland, during HUMPPA-COPEC 2010, *Atmos. Chem.*
740 *Phys.*, 13, 12233–12256, doi:10.5194/acp-13-12233-2013, 2013.
741
- 742 Dal Maso M., Sogacheva L., Anisimov M. P., Arshinov M., Baklanov A., Belan B., Khodzher T.
743 V., Obolkin V. A., Staroverova A., Vlasov A., Zagaynov V. A., Lushnikov A., Lyubovtseva Y. S.,
744 Riipinen I., Kerminen V.-M. and Kulmala M.: Aerosol particle formation events at two Siberian
745 stations inside the boreal forest. *Boreal Env. Res.* 13, 81–92, 2008.
746
- 747 Denier van der Gon, H., Visschedijk, A., Johansson, C., Hedberg Larsson, E., Harrison, R. M.,
748 and Beddows, D.: Size-resolved Pan European Anthropogenic Particle Number Inventory,
749 EUCAARI Deliverable 141, 2009.
750

751 Denier van der Gon, H., Visschedijk, A., Johansson, C., Ntziachristos, L., and Harrison, R. M.:
752 Size-resolved Pan-European Anthropogenic Particle Number Inventory, paper presented at
753 International Aerosol conference (oral), 29 August 3 September 2010, Helsinki, 2010.
754

755 Dentener, F., Kinne, S., Bond, T., Boucher, O., Cofala, J., Generoso, S., Ginoux, P., Gong, S.,
756 Hoelzemann, J. J., Ito, A., Marelli, L., Penner, J. E., Putaud, J.-P., Textor, C., Schulz, M., van der
757 Werf, G. R., and Wilson, J.: Emissions of primary aerosol and precursor gases in the years
758 2000 and 1750 prescribed data-sets for AeroCom, *Atmos. Chem. Phys.*, 6, 4321-4344,
759 doi:10.5194/acp-6-4321-2006, 2006.
760

761 Forster, P., Ramaswamy, V., Artaxo, P., Berntsen, T., Betts, R., Fahey, D.W., Haywood, J., Lean,
762 J., Lowe, D.C., Myhre, G., Nganga, J., Prinn, R., Raga, G., Schulz, M., Van Dorland, R. and
763 Miller, H.L.: *Changes in Atmospheric Constituents and in Radiative Forcing Chapter 2*. United
764 Kingdom: Cambridge University Press, 2007.
765

766 Guenther, A., Karl, T., Harley, P., Wiedinmyer, C., Palmer, P. I., and Geron, C.: Estimates of
767 global terrestrial isoprene emissions using MEGAN (Model of Emissions of Gases and
768 Aerosols from Nature), *Atmos. Chem. Phys.*, 6, 3181-3210, doi:10.5194/acp-6- 3181-2006,
769 2006.
770

771 Gultepe, I. Isaac, G.A.: Scale Effects on Averaging of Cloud Droplet and Aerosol Number
772 Concentrations: Observations and Models. *J. Climate* 12:1268-1279, 1999.
773

774 Hamed, A., Joutsensaari, J., Mikkonen, S., Sogacheva, L., Dal Maso, M., Kulmala, M., Cavalli,
775 F., Fuzzi, S., Facchini, M. C., Decesari, S., Mircea, M., Lehtinen, K. E. J., and Laaksonen, A.:
776 Nucleation and growth of new particles in Po Valley, Italy, *Atmos. Chem. Phys.*, 7, 355-376,
777 doi:10.5194/acp-7-355-2007, 2007.

778 Hari P., Kulmala M., Pohja T., Lahti T., Siivola E., Palva L., Aalto P., Hämeri K., Vesala T.,
779 Luoma S. and Pulliainen E.: Air pollution in Eastern Lapland: challenge for an
780 environmental measurement station. *Silva Fennica* 28: 29-39, 1994.

781 Hari, P. & Kulmala, M. Station for Measuring Ecosystem-Atmosphere Relations (SMEAR II).
782 *Boreal Env. Res.*, 10, 315-322, 2005.

783 Herrmann, E., Ding, A. J., Kerminen, V.-M., Petäjä, T., Yang, X. Q., Sun, J. N., Qi, X. M.,
784 Manninen, H., Hakala, J., Nieminen, T., Aalto, P. P., Kulmala, M., and Fu, C. B.: Aerosols and
785 nucleation in eastern China: first insights from the new SORPES-NJU station, *Atmos. Chem.*
786 *Phys.*, 14, 2169-2183, doi:10.5194/acp-14-2169-2014, 2014.
787

788 Hinds, W. C. (1982) *Aerosol Technology*, p. 85. Wiley, New York.
789

790 IPCC, *Climate Change: The Physical Science Basis. Contribution of Working Group I to the*
791 *Fifth Assessment Report of the Intergovernmental Panel on Climate Change* [Stocker, T.F., D.
792 Qin, G.-K. Plattner, M. Tignor, S.K. Allen, J. Boschung, A. Nauels, Y. Xia, V. Bex and P.M.
793 Midgley (eds.)]. Cambridge University Press, Cambridge, United Kingdom and New York, NY,
794 USA, 1535 pp, doi:10.1017/CBO9781107415324, 2013.
795

796 Jones, A., Haywood, J. M. and Boucher, O.: Aerosol forcing, climate response and climate
797 sensitivity in the Hadley Centre climate model, *J. Geophys. Res.*, 112, D20211,
798 doi:10.1029/2007JD008688, 2007.
799

800 Jokinen, T., Berndt, T., Makkonen, R., Kerminen, V., Junninen, H., Paasonen, P., Stratmann, F.,
801 Herrmann, H., Guenther, A.B., Worsnop, D.R., Kulmala, M., Ehn, M., Sipilä, M.: Production of
802 extremely low volatile organic compounds from biogenic emissions: Measured yields and
803 atmospheric implications, *Proceedings of the National Academy of Sciences* 112:7123-7128,
804 2015.
805
806 Kazil, J., Stier, P., Zhang, K., Quaas, J., Kinne, S., O'Donnell, D., Rast, S., Esch, M., Ferrachat,
807 S., Lohmann, U., and Feichter, J.: Aerosol nucleation and its role for clouds and Earth's
808 radiative forcing in the aerosol-climate model ECHAM5-HAM, *Atmos. Chem. Phys.*, 10,
809 10733-10752, doi:10.5194/acp-10-10733-2010, 2010.
810
811 Kerminen, V.-M., Kulmala, M.: Analytical formulae connecting the "real" and the "apparent"
812 nucleation rate and the nuclei number concentration for atmospheric nucleation events. *J*
813 *Aerosol Sci* 33(4):609-622, 2002.
814
815 Kerminen, V.-M., Paramonov, M., Anttila, T., Riipinen, I., Fountoukis, C., Korhonen, H., Asmi,
816 E., Laakso, L., Lihavainen, H., Swietlicki, E., Svenningsson, B., Asmi, A., Pandis, S. N.,
817 Kulmala, M., and Petäjä, T.: Cloud condensation nuclei production associated with
818 atmospheric nucleation: a synthesis based on existing literature and new results, *Atmos.*
819 *Chem. Phys.*, 12, 12037-12059, doi:10.5194/acp-12-12037-2012, 2012.
820
821 Kinne, S., Schulz, M., Textor, C., Guibert, S., Balkanski, Y., Bauer, S. E., Berntsen, T., Berglen,
822 T. F., Boucher, O., Chin, M., Collins, W., Dentener, F., Diehl, T., Easter, R., Feichter, J., Fillmore,
823 D., Ghan, S., Ginoux, P., Gong, S., Grini, A., Hendricks, J., Herzog, M., Horowitz, L., Isaksen, I.,
824 Iversen, T., Kirkevåg, A., Kloster, S., Koch, D., Kristjansson, J. E., Krol, M., Lauer, A.,
825 Lamarque, J. F., Lesins, G., Liu, X., Lohmann, U., Montanaro, V., Myhre, G., Penner, J., Pitari,
826 G., Reddy, S., Seland, O., Stier, P., Takemura, T., and Tie, X.: An AeroCom initial assessment –
827 optical properties in aerosol component modules of global models, *Atmos. Chem. Phys.*, 6,
828 1815-1834, doi:10.5194/acp-6-1815-2006, 2006.
829
830 Kiss, G., Varga, B., Galambos, I., & Ganszky, I. Characterization of water-soluble organic
831 matter isolated from atmospheric fine aerosol. *J. Geophys. Res.*, 107, 8339-8347,
832 doi:10.1029/2001JD000603, 2002.
833
834 Klimont, Z., Kupiainen, K., Heyes, C., Purohit, P., Cofala, J., Rafaj, P., Borcken-Kleefeld, J. and
835 Schöpp, W.: Global anthropogenic emissions of particulate matter including black carbon,
836 *Atmospheric Chem. Phys. Discuss.*, 2016, 1-72, doi:10.5194/acp-2016-880, 2016.
837
838 Kloster, S., Feichter, J., Maier-Reimer, E., Six, K. D., Stier, P., and Wetzzel, P.: DMS cycle in the
839 marine ocean-atmosphere system – a global model study, *Biogeosciences*, 3, 29-51,
840 doi:10.5194/bg-3-29-2006, 2006.
841
842 Kooperman, G. J., Pritchard, M. S., Ghan, S. J., Wang, M., Somerville, R. C. J., and Russell, L.
843 M.: Constraining the influence of natural variability to improve estimates of global aerosol
844 indirect effects in a nudged version of the Community Atmosphere Model 5, *J. Geophys. Res.*,
845 117, D23204, doi:10.1029/2012JD018588, 2012.
846
847 Kulmala, M., Dal Maso, M., Mäkelä, J., Pirjola, L., Väkevä, M., Aalto, P., Miikkulainen, P.,
848 Hämeri, K., and O'dowd, C.: On the formation, growth and composition of nucleation mode
849 particles. *Tellus B*, 53(4). doi:http://dx.doi.org/10.3402/tellusb.v53i4.16622, 2001.

850

851 Kupiainen, K. and Klimont, Z.: Primary emissions of fine carbonaceous particles in Europe.
852 Atmospheric Environment 41:2156 – 2170, 2007.
853

854 Laakso, L., Laakso, H., Aalto, P. P., Keronen, P., Petäjä, T., Nieminen, T., Pohja, T., Siivola, E.,
855 Kulmala, M., Kgabi, N., Molefe, M., Mabaso, D., Phalatse, D., Pienaar, K., and Kerminen, V.-M.:
856 Basic characteristics of atmospheric particles, trace gases and meteorology in a relatively
857 clean Southern African Savannah environment, Atmos. Chem. Phys., 8, 4823-4839,
858 doi:10.5194/acp-8-4823-2008, 2008.
859

860 Lee, L. A., Pringle, K. J., Reddington, C. L., Mann, G. W., Stier, P., Spracklen, D. V., Pierce, J. R.,
861 and Carslaw, K. S.: The magnitude and causes of uncertainty in global model simulations of
862 cloud condensation nuclei, Atmos. Chem. Phys., 13, 8879-8914, doi:10.5194/acp-13-8879-
863 2013, 2013.
864

865 Liao, L., Kerminen, V.-M., Boy, M., Kulmala, M., and Dal Maso, M.: Temperature influence on
866 the natural aerosol budget over boreal forests, Atmos. Chem. Phys., 14, 8295-8308,
867 doi:10.5194/acp-14-8295-2014, 2014.
868

869 Lohmann, U. and Feichter, J.: Global indirect aerosol effects: a review, Atmos. Chem. Phys.,
870 5, 715-737, doi:10.5194/acp-5-715-2005, 2005.
871

872 Luo, G. and Yu, F.: Sensitivity of global cloud condensation nuclei concentrations to primary
873 sulfate emission parameterizations, Atmos. Chem. Phys., 11, 1949-1959,
874 <https://doi.org/10.5194/acp-11-1949-2011>, 2011.
875

876 Makkonen, R., Asmi, A., Korhonen, H., Kokkola, H., Järvenoja, S., Räisänen, P., Lehtinen, K. E.
877 J., Laaksonen, A., Kerminen, V.-M., Järvinen, H., Lohmann, U., Bennartz, R., Feichter, J., and
878 Kulmala, M.: Sensitivity of aerosol concentrations and cloud properties to nucleation and
879 secondary organic distribution in ECHAM5-HAM global circulation model, Atmos. Chem.
880 Phys., 9, 1747-1766, doi:10.5194/acp-9-1747-2009, 2009.
881

882 Makkonen, R., Asmi, A., Kerminen, V.-M., Boy, M., Arneth, A., Guenther, A., and Kulmala, M.:
883 BVOC-aerosol-climate interactions in the global aerosol-climate model ECHAM5.5-HAM2,
884 Atmos. Chem. Phys., 12, 10077-10096, doi:10.5194/acp-12-10077-2012, 2012.
885

886 Merikanto, J., Spracklen, D. V., Mann, G. W., Pickering, S. J., and Carslaw, K. S.: Impact of
887 nucleation on global CCN, Atmos. Chem. Phys., 9, 8601-8616, doi:10.5194/acp-9-8601-2009,
888 2009.
889

890 Paasonen, P., Asmi, A., Petaja, T., Kajos, M.K, Aijala, M, Junninen, H, Holst, T, Abbatt, J.P.D,
891 Arneth, A, Birmili, W, van der Gon, H.D, Hamed, A, Hoffer, A, Laakso, L, Laaksonen, A,
892 Richard Leaitch, W, Plass-Dulmer, C, Pryor, S.C, Raisanen, P, Swietlicki, E, Wiedensohler, A,
893 Worsnop, D.R, Kerminen, V, Kulmala, M.: Warming-induced increase in aerosol number
894 concentration likely to moderate climate change. Nature Geoscience 6:438-442, 2013.
895

896 Paasonen, P., Kupiainen, K., Klimont, Z., Visschedijk, A., Denier van der Gon, H. A. C., and
897 Amann, M.: Continental anthropogenic primary particle number emissions, Atmos. Chem.
898 Phys., 16, 6823-6840, doi:10.5194/acp-16-6823-2016, 2016.
899

900 Pozzoli, L., Janssens-Maenhout, G., Diehl, T., Bey, I., Schultz, M. G., Feichter, J., Vignati, E.,
901 and Dentener, F.: Re-analysis of tropospheric sulfate aerosol and ozone for the period 1980-
902 2005 using the aerosol-chemistry-climate model ECHAM5-HAMMOZ, Atmos. Chem. Phys., 11,
903 9563-9594, doi:10.5194/acp-11-9563-2011, 2011.

904
905 Riipinen, I., Pierce, J. R., Yli-Juuti, T., Nieminen, T., Häkkinen, S., Ehn, M., Junninen, H.,
906 Lehtipalo, K., Petäjä, T., Slowik, J., Chang, R., Shantz, N. C., Abbatt, J., Leaitch, W. R.,
907 Kerminen, V.-M., Worsnop, D. R., Pandis, S. N., Donahue, N. M., and Kulmala, M.: Organic
908 condensation: a vital link connecting aerosol formation to cloud condensation nuclei (CCN)
909 concentrations, *Atmos. Chem. Phys.*, 11, 3865-3878, doi:10.5194/acp-11-3865-2011, 2011.
910
911 Roelofs, G.-J., ten Brink, H., Kiendler-Scharr, A., de Leeuw, G., Mensah, A., Minikin, A., and
912 Otjes, R.: Evaluation of simulated aerosol properties with the aerosol-climate model
913 ECHAM5-HAM using observations from the IMPACT field campaign, *Atmos. Chem. Phys.*, 10,
914 7709-7722, doi:10.5194/acp-10-7709-2010, 2010.
915
916 Ruuskanen, T. M., Kaasik, M., Aalto, P. P., Hörrak, U., Vana, M., Mårtensson, M., Yoon, Y. J.,
917 Keronen, P., Mordas, G., Ceburnis, D., Nilsson, E. D., O'Dowd, C., Noppel, M., Alliksaar, T.,
918 Ivask, J., Sofiev, M., Prank, M., and Kulmala, M.: Concentrations and fluxes of aerosol
919 particles during the LAPBIAT measurement campaign at Värriö field station, *Atmos. Chem.*
920 *Phys.*, 7, 3683-3700, doi:10.5194/acp-7-3683-2007, 2007.
921
922 Samset, B. H., Myhre, G., Herber, A., Kondo, Y., Li, S.-M., Moteki, N., Koike, M., Oshima, N.,
923 Schwarz, J. P., Balkanski, Y., Bauer, S. E., Bellouin, N., Bernsten, T. K., Bian, H., Chin, M., Diehl,
924 T., Easter, R. C., Ghan, S. J., Iversen, T., Kirkevåg, A., Lamarque, J.-F., Lin, G., Liu, X., Penner, J.
925 E., Schulz, M., Seland, Ø., Skeie, R. B., Stier, P., Takemura, T., Tsigaridis, K., and Zhang, K.:
926 Modelled black carbon radiative forcing and atmospheric lifetime in AeroCom Phase II
927 constrained by aircraft observations, *Atmos. Chem. Phys.*, 14, 12465-12477,
928 doi:10.5194/acp-14-12465-2014, 2014.
929
930 Schulz, M., Textor, C., Kinne, S., Balkanski, Y., Bauer, S., Bernsten, T., Berglen, T., Boucher, O.,
931 Dentener, F., Guibert, S., Isaksen, I. S. A., Iversen, T., Koch, D., Kirkevåg, A., Liu, X.,
932 Montanaro, V., Myhre, G., Penner, J. E., Pitari, G., Reddy, S., Seland, Ø., Stier, P., and
933 Takemura, T.: Radiative forcing by aerosols as derived from the AeroCom present-day and
934 pre-industrial simulations, *Atmos. Chem. Phys.*, 6, 5225-5246, doi:10.5194/acp-6-5225-2006,
935 2006.
936
937 Schurgers, G., Arneth, A., Holzinger, R., and Goldstein, A. H.: Process-based modelling of
938 biogenic monoterpene emissions combining production and release from storage, *Atmos.*
939 *Chem. Phys.*, 9, 3409-3423, doi:10.5194/acp-9-3409-2009, 2009.
940
941 Schutgens, N. A. J., Gryspeerdt, E., Weigum, N., Tsyro, S., Goto, D., Schulz, M., and Stier, P.:
942 Will a perfect model agree with perfect observations? The impact of spatial sampling, *Atmos.*
943 *Chem. Phys.*, 16, 6335-6353, doi:10.5194/acp-16-6335-2016, 2016.
944
945 Seinfeld, J. H. and Pandis, S. N.: *Atmospheric Chemistry and Physics: From Air Pollution to*
946 *Climate Change*, John Wiley and Sons, 1998.
947
948 Shilling, J. E., Zaveri, R. A., Fast, J. D., Kleinman, L., Alexander, M. L., Canagaratna, M. R.,
949 Fortner, E., Hubbe, J. M., Jayne, J. T., Sedlacek, A., Setyan, A., Springston, S., Worsnop, D. R.,
950 and Zhang, Q.: Enhanced SOA formation from mixed anthropogenic and biogenic emissions
951 during the CARES campaign, *Atmos. Chem. Phys.*, 13, 2091-2113, doi:10.5194/acp-13-2091-
952 2013, 2013.
953
954 Shindell, D. T., Faluvegi, G., Bauer, S. E., Koch, D. M., Unger, N., Menon, S., Miller, R. L.,
955 Schmidt, G. A. and Streets, D. G.: Climate response to projected changes in short-lived

956 species under an A1B scenario from 2000–2050 in the GISS climate model, *J. Geophys. Res.*,
957 112, D20103, doi:10.1029/2007JD008753, 2007.

958

959 Spracklen, D. V., Carslaw, K. S., Kulmala, M., Kerminen, V.-M., Mann, G. W., and Sihto, S.-L.:
960 The contribution of boundary layer nucleation events to total particle concentrations on
961 regional and global scales, *Atmos. Chem. Phys.*, 6, 5631-5648, doi:10.5194/acp-6-5631-
962 2006, 2006.

963

964 Spracklen, D. V., Carslaw, K. S., Kerminen, V.-M., Sihto, S.-L., Riipinen, I., Merikanto, J., Mann,
965 G. W., Chipperfield, M. P., Wiedensohler, A., Birmili, W. and Lihavainen, H.: Contribution of
966 particle formation to global cloud condensation nuclei concentrations, *Geophys. Res. Lett.*,
967 35, L06808, doi:10.1029/2007GL033038.

968

969 Spracklen, D. V., Carslaw, K. S., Merikanto, J., Mann, G. W., Reddington, C. L., Pickering, S.,
970 Ogren, J. A., Andrews, E., Baltensperger, U., Weingartner, E., Boy, M., Kulmala, M., Laakso, L.,
971 Lihavainen, H., Kivekäs, N., Komppula, M., Mihalopoulos, N., Kouvarakis, G., Jennings, S. G.,
972 O'Dowd, C., Birmili, W., Wiedensohler, A., Weller, R., Gras, J., Laj, P., Sellegri, K., Bonn, B.,
973 Krejci, R., Laaksonen, A., Hamed, A., Minikin, A., Harrison, R. M., Talbot, R., and Sun, J.:
974 Explaining global surface aerosol number concentrations in terms of primary emissions and
975 particle formation, *Atmos. Chem. Phys.*, 10, 4775-4793, doi:10.5194/acp-10-4775-2010,
976 2010.

977

978 Spracklen, D. V., Jimenez, J. L., Carslaw, K. S., Worsnop, D. R., Evans, M. J., Mann, G. W.,
979 Zhang, Q., Canagaratna, M. R., Allan, J., Coe, H., McFiggans, G., Rap, A., and Forster, P.:
980 Aerosol mass spectrometer constraint on the global secondary organic aerosol budget,
981 *Atmos. Chem. Phys.*, 11, 12109-12136, doi:10.5194/acp-11-12109-2011, 2011.

982

983 Stevens, R. G. and Pierce, J. R.: A parameterization of sub-grid particle formation in sulfur-
984 rich plumes for global- and regional-scale models, *Atmos. Chem. Phys.*, 13, 12117-12133,
985 doi:10.5194/acp-13-12117-2013, 2013.

986

987 Stier, P., Feichter, J., Kinne, S., Kloster, S., Vignati, E., Wilson, J., Ganzeveld, L., Tegen, I.,
988 Werner, M., Balkanski, Y., Schulz, M., Boucher, O., Minikin, A., and Petzold, A.: The aerosol-
989 climate model ECHAM5-HAM, *Atmos. Chem. Phys.*, 5, 1125-1156, doi:10.5194/acp-5-1125-
990 2005, 2005.

991

992 Stier, P., Seinfeld, J. H., Kinne, S., and Boucher, O.: Aerosol absorption and radiative forcing,
993 *Atmos. Chem. Phys.*, 7, 5237-5261, doi:10.5194/acp-7-5237-2007, 2007.

994

995 Stohl, A., Aamaas, B., Amann, M., Baker, L. H., Bellouin, N., Berntsen, T. K., Boucher, O.,
996 Cherian, R., Collins, W., Daskalakis, N., Dusinska, M., Eckhardt, S., Fuglestad, J. S., Harju,
997 M., Heyes, C., Hodnebrog, Ø., Hao, J., Im, U., Kanakidou, M., Klimont, Z., Kupiainen, K., Law,
998 K. S., Lund, M. T., Maas, R., MacIntosh, C. R., Myhre, G., Myriokefalitakis, S., Olivíe, D., Quaas,
999 J., Quennehen, B., Raut, J.-C., Rumbold, S. T., Samset, B. H., Schulz, M., Seland, Ø., Shine, K.
1000 P., Skeie, R. B., Wang, S., Yttri, K. E., and Zhu, T.: Evaluating the climate and air quality
1001 impacts of short-lived pollutants, *Atmos. Chem. Phys.*, 15, 10529-10566, doi:10.5194/acp-
1002 15-10529-2015, 2015.

1003

1004 Textor, C., Schulz, M., Guibert, S., Kinne, S., Balkanski, Y., Bauer, S., Berntsen, T., Berglen, T.,
1005 Boucher, O., Chin, M., Dentener, F., Diehl, T., Easter, R., Feichter, H., Fillmore, D., Ghan, S.,
1006 Ginoux, P., Gong, S., Grini, A., Hendricks, J., Horowitz, L., Huang, P., Isaksen, I., Iversen, I.,
1007 Kloster, S., Koch, D., Kirkevåg, A., Kristjansson, J. E., Krol, M., Lauer, A., Lamarque, J. F., Liu,
1008 X., Montanaro, V., Myhre, G., Penner, J., Pitari, G., Reddy, S., Seland, Ø., Stier, P., Takemura,

1009 T., and Tie, X.: Analysis and quantification of the diversities of aerosol life cycles within
1010 AeroCom, *Atmos. Chem. Phys.*, 6, 1777-1813, doi:10.5194/acp-6-1777-2006, 2006.
1011
1012 Tonttila, J., Järvinen, H., and Räisänen, P.: Explicit representation of subgrid variability in
1013 cloud microphysics yields weaker aerosol indirect effect in the ECHAM5-HAM2 climate model,
1014 *Atmos. Chem. Phys.*, 15, 703-714, doi:10.5194/acp-15-703-2015, 2015.
1015
1016 Tsigaridis, K., Daskalakis, N., Kanakidou, M., Adams, P. J., Artaxo, P., Bahadur, R., Balkanski,
1017 Y., Bauer, S. E., Bellouin, N., Benedetti, A., Bergman, T., Berntsen, T. K., Beukes, J. P., Bian, H.,
1018 Carslaw, K. S., Chin, M., Curci, G., Diehl, T., Easter, R. C., Ghan, S. J., Gong, S. L., Hodzic, A.,
1019 Hoyle, C. R., Iversen, T., Jathar, S., Jimenez, J. L., Kaiser, J. W., Kirkevåg, A., Koch, D., Kokkola,
1020 H., Lee, Y. H., Lin, G., Liu, X., Luo, G., Ma, X., Mann, G. W., Mihalopoulos, N., Morcrette, J.-J.,
1021 Müller, J.-F., Myhre, G., Myriokefalitakis, S., Ng, N. L., O'Donnell, D., Penner, J. E., Pozzoli, L.,
1022 Pringle, K. J., Russell, L. M., Schulz, M., Sciare, J., Seland, Ø., Shindell, D. T., Sillman, S., Skeie,
1023 R. B., Spracklen, D., Stavroukou, T., Steenrod, S. D., Takemura, T., Tiitta, P., Tilmes, S., Tost, H.,
1024 van Noije, T., van Zyl, P. G., von Salzen, K., Yu, F., Wang, Z., Wang, Z., Zaveri, R. A., Zhang,
1025 H., Zhang, K., Zhang, Q., and Zhang, X.: The AeroCom evaluation and intercomparison of
1026 organic aerosol in global models, *Atmos. Chem. Phys.*, 14, 10845-10895, doi:10.5194/acp-
1027 14-10845-2014, 2014.
1028
1029 Turpin, B.J., Saxena, P., Andrews, E.: Measuring and simulating particulate organics in the
1030 atmosphere: problems and prospects. *Atmospheric Environment* 34:2983-3013, 2000.
1031
1032 van Ulden, A. and Wieringa, J.: Atmospheric boundary layer re- search at Cabauw, Bound.-
1033 Lay. Meteorol., 78, 39-69, 1996.
1034
1035 Vignati, E., Wilson, J. and Stier, P.: M7: An efficient size-resolved aerosol microphysics module
1036 for large-scale aerosol transport models, *J. Geophys. Res.*, 109, D22202,
1037 doi:10.1029/2003JD004485, 2004.
1038
1039 Zhang, K., O'Donnell, D., Kazil, J., Stier, P., Kinne, S., Lohmann, U., Ferrachat, S., Croft, B.,
1040 Quaas, J., Wan, H., Rast, S., and Feichter, J.: The global aerosol-climate model ECHAM-HAM,
1041 version 2: sensitivity to improvements in process representations, *Atmos. Chem. Phys.*, 12,
1042 8911-8949, doi:10.5194/acp-12-8911-2012, 2012.
1043
1044 Zhang, S., Wang, M., Ghan, S. J., Ding, A., Wang, H., Zhang, K., Neubauer, D., Lohmann, U.,
1045 Ferrachat, S., Takeamura, T., Gettelman, A., Morrison, H., Lee, Y., Shindell, D. T., Partridge, D.
1046 G., Stier, P., Kipling, Z., and Fu, C.: On the characteristics of aerosol indirect effect based on
1047 dynamic regimes in global climate models, *Atmos. Chem. Phys.*, 16, 2765-2783,
1048 doi:10.5194/acp-16-2765-2016, 2016.
1049
1050
1051
1052
1053
1054
1055
1056
1057
1058
1059

TABLES

1060
1061
1062
1063
1064
1065
1066

Table 1. Input data provided from AeroCom and GAINS inventories for submicron particle emissions. The data is sorted according to its original structure in terms of mass, number, chemical species differentiation (BC, OC and SO₄), bi-level vertical distribution (2-zL) and base year. (✓) and (x) indicate whether the inventory contains a certain information or not, respectively.

Data	M	N	Species	2-zL	Year
AeroCom	✓	x	✓	✓	2000
GAINS	x	✓	x	x	2010

1067
1068
1069
1070
1071
1072
1073
1074
1075
1076
1077
1078
1079
1080
1081
1082
1083
1084

1085 Table 2. Description of measurement sites for model versus observation evaluation.

Station	Lon	Lat	m. a. s. l.	Years	Reference
Botsalano, South Africa	25.8 ° E	25.5 ° S	1424	07/2006-08/2007	Laakso et al., 2008.
Cabauw, Netherlands	4.9 ° E	52.0 ° N	60	04/2008-03/2009	van Ulden and Wieringa, 1996.
Hohenpeissenberg, Germany	11.0 ° E	47.8 ° N	980	06/2007-11/2008	Birmili et al., 2016.
Hyytiälä, Finland	24.3 ° E	61.9 ° N	180	01/2009-12/2010	Hari and Kulmala, 2005.
K-Pusztá, Hungary	19.6 ° E	47.0 ° N	125	03/2007-03/2009	Kiss et al., 2002.
Melpitz, Germany	12.9 ° E	51.5 ° N	84	01/2007-12/2008	Birmili et al., 2016.
Nanjing, China	118.9 ° E	32.1 ° N	40	12/2011-12/2014	Herrmann et al., 2014.
Po Valley, Italy	11.6 ° E	44.7 ° N	11	09/2004-09/2006	Hamed et al., 2007.
Sao Paulo, Brazil	46.7 ° W	23.5 ° S	760	10/2010-09/2011	Backman et al., 2012.
Tomsk FNV, Russia	84.1 ° E	56.4 ° N	80	01/2012-12/2013	Dal Maso et al., 2008.
Värriö, Finland	29.6 ° E	67.8 ° N	400	01/2009-12/2011	Hari et al., 1994.

1086

1087 Table 3. Annual total anthropogenic particle number emissions (second and third columns)
 1088 and respective global average ratios (fourth and fifth columns) computed for the whole
 1089 domain. R_{tot} ratios are calculated by firstly averaging the emissions among the whole domain
 1090 for each data set, and secondly divide GAINS by AeroCom. This method aims at studying
 1091 absolute differences in the global emissions with no regard to geographical distribution
 1092 differences. In R_{grid} we firstly divide the data sets to keep the information of data sets
 1093 differences for each grid cell, and secondly compute the median of gridded ratios. R_{grid} is
 1094 weighted by surface area of the grid cell.

Global emissions	AeroCom 10^{25} yr^{-1}	GAINS 10^{25} yr^{-1}	R_{tot} mean	R_{grid} median
Total	3.42	7.39	2.16	1.00
Accumulation	0.028	1.74	62.14	48.65
Aitken	3.39	5.66	1.67	0.71

1095

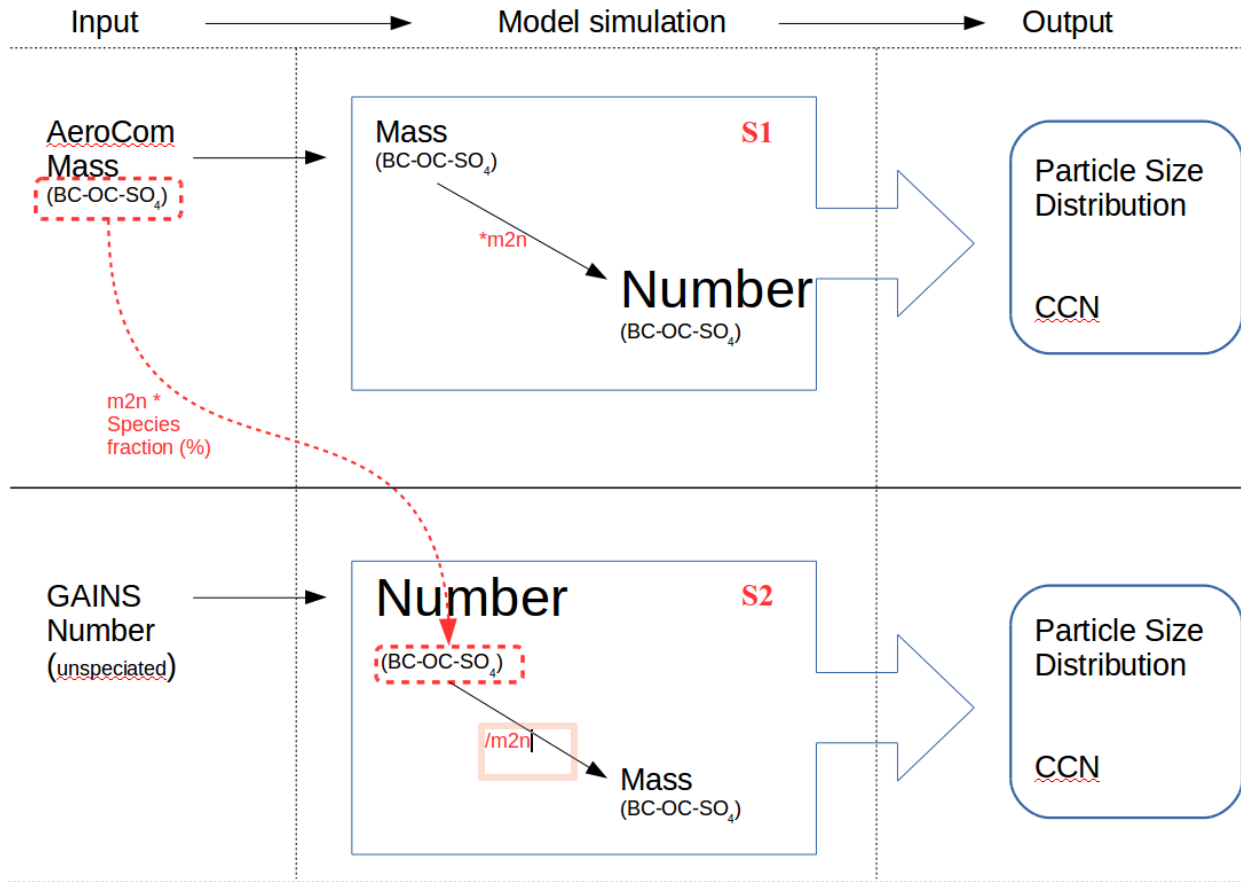
1096 Table 4. Modeled global annually-averaged concentrations of total anthropogenic particles at
 1097 surface level, CCN0.2 and CCN1,0 with AeroCom and GAINS (second and third columns).
 1098 Continental and (global) average ratios of total particles and CCN concentrations were
 1099 calculated as in Table 3.
 1100

Global concentrations	AeroCom 10^8 m^{-3}	GAINS 10^8 m^{-3}	R_{tot} mean	R_{grid} median
Total	37.08	33.98	0.83 (0.91)	0.96 (0.99)
CCN0.2	1.65	2.47	1.69 (1.49)	1.16 (1.04)
CCN1.0	7.04	6.77	0.96 (0.96)	0.99 (0.98)

1101
 1102
 1103
 1104
 1105
 1106
 1107
 1108
 1109
 1110
 1111
 1112

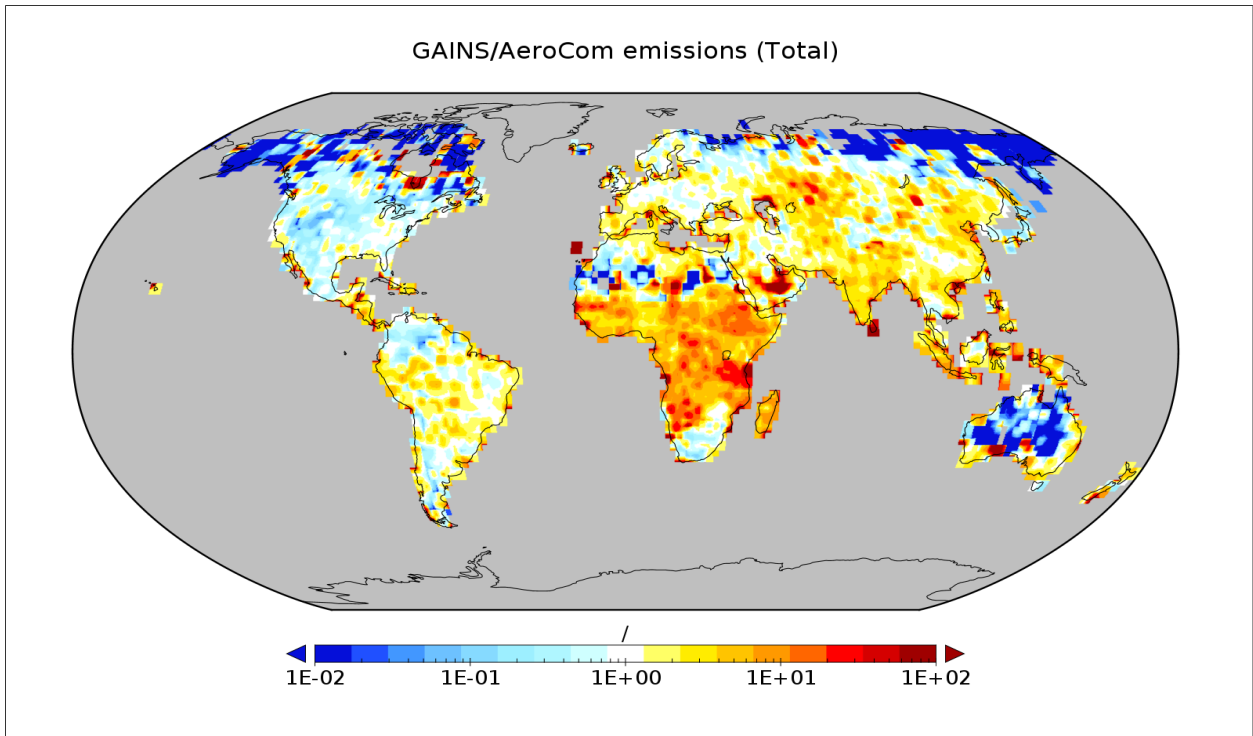
1113
1114

FIGURES



1116 Figure 1. Framework describing the off-line steps to implement GAINS mass and number
1117 anthropogenic emissions in the ECHAM-HAM. The AeroCom mass-to-number (m2n)
1118 conversion factors and the chemical species fractions (%) of AeroCom number emissions
1119 were used to speciate GAINS number emissions. A specific m2n factor was used for each
1120 species for either mass-to-number (*m2n) or number-to-mass (/m2n) conversion.

1121
1122
1123
1124
1125
1126
1127
1128



1129 Figure 2. GAINS/AeroCom ratio for annual anthropogenic particle number emissions.

1130

1131

1132

1133

1134

1135

1136

1137

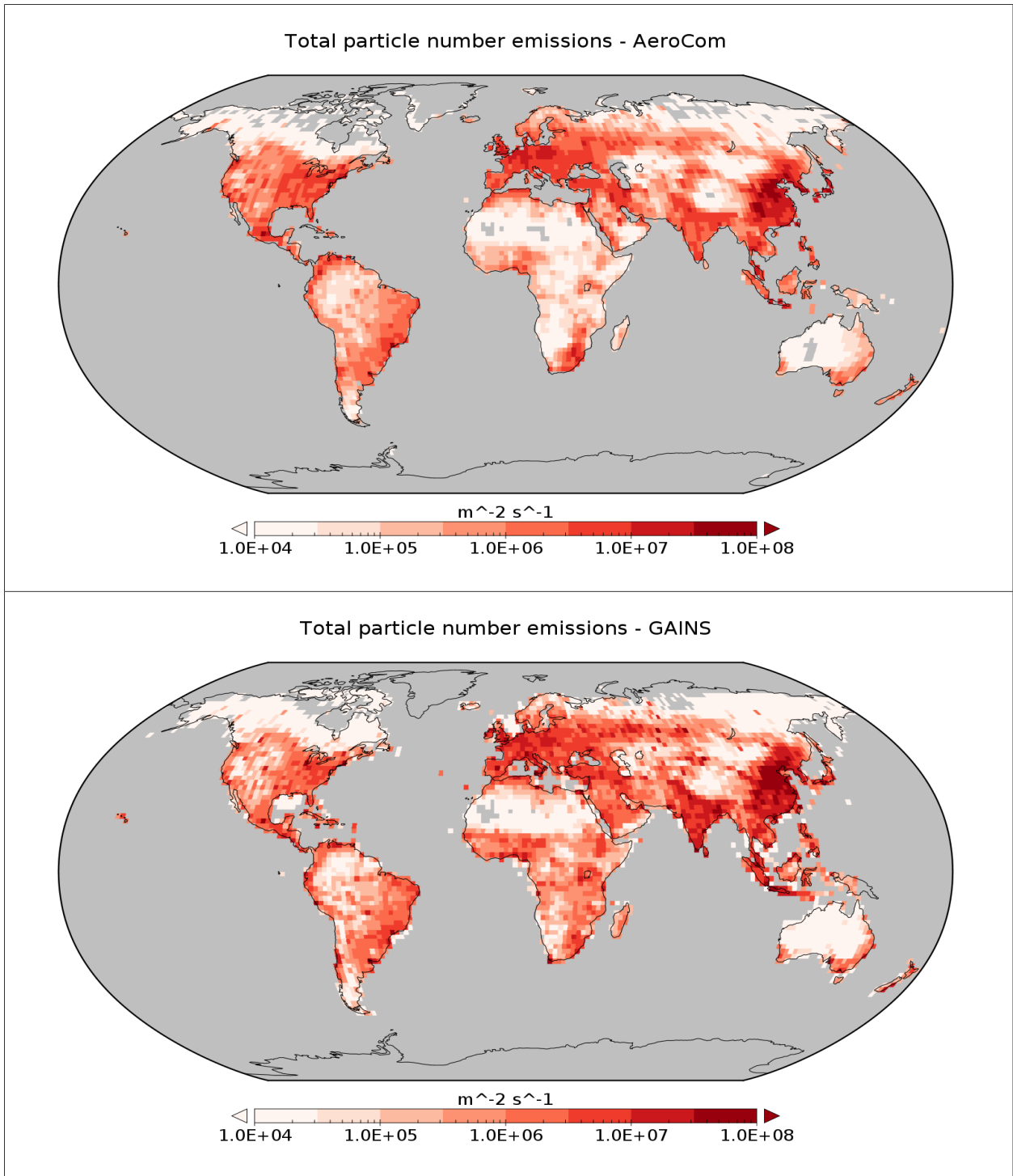
1138

1139

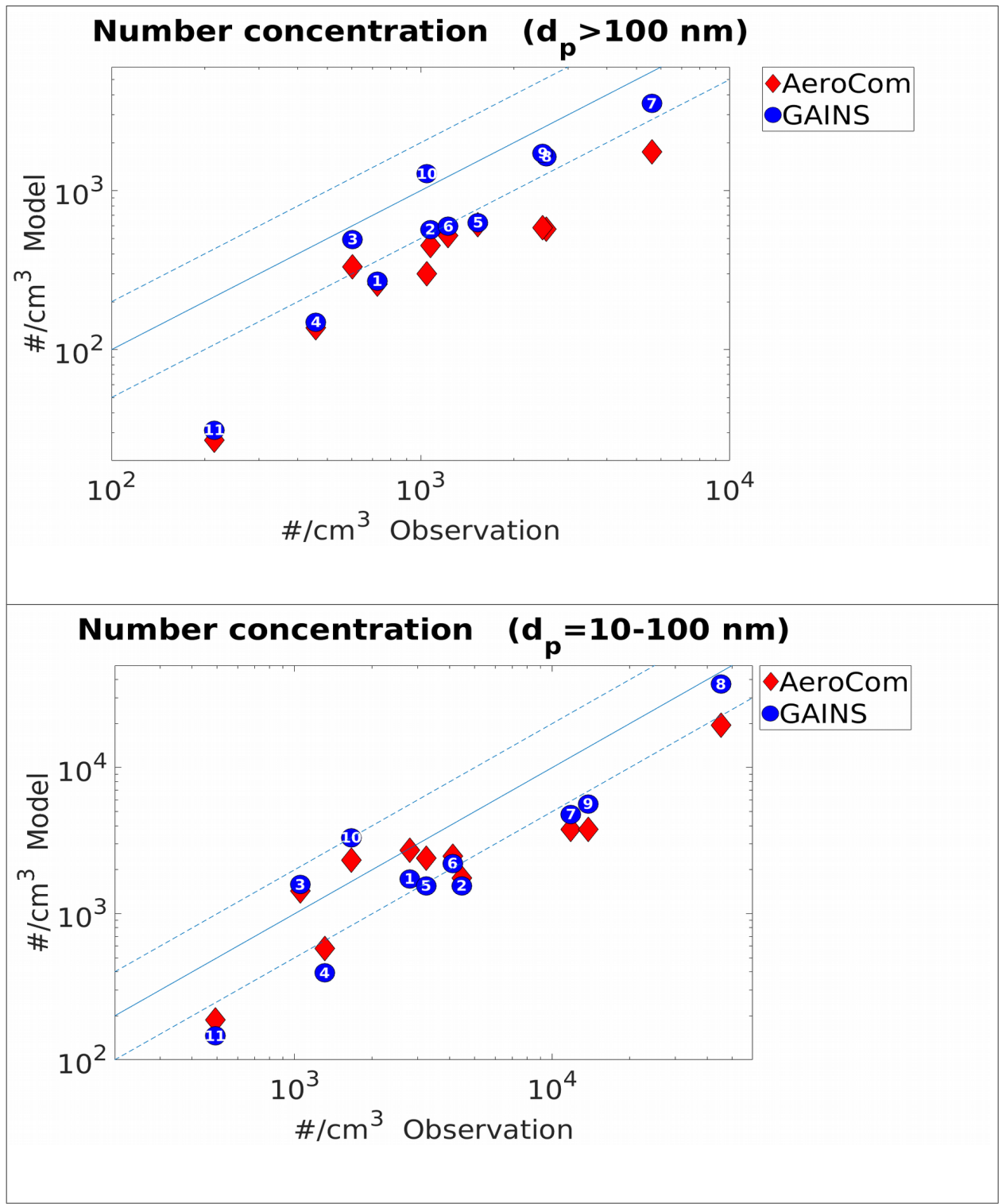
1140

1141

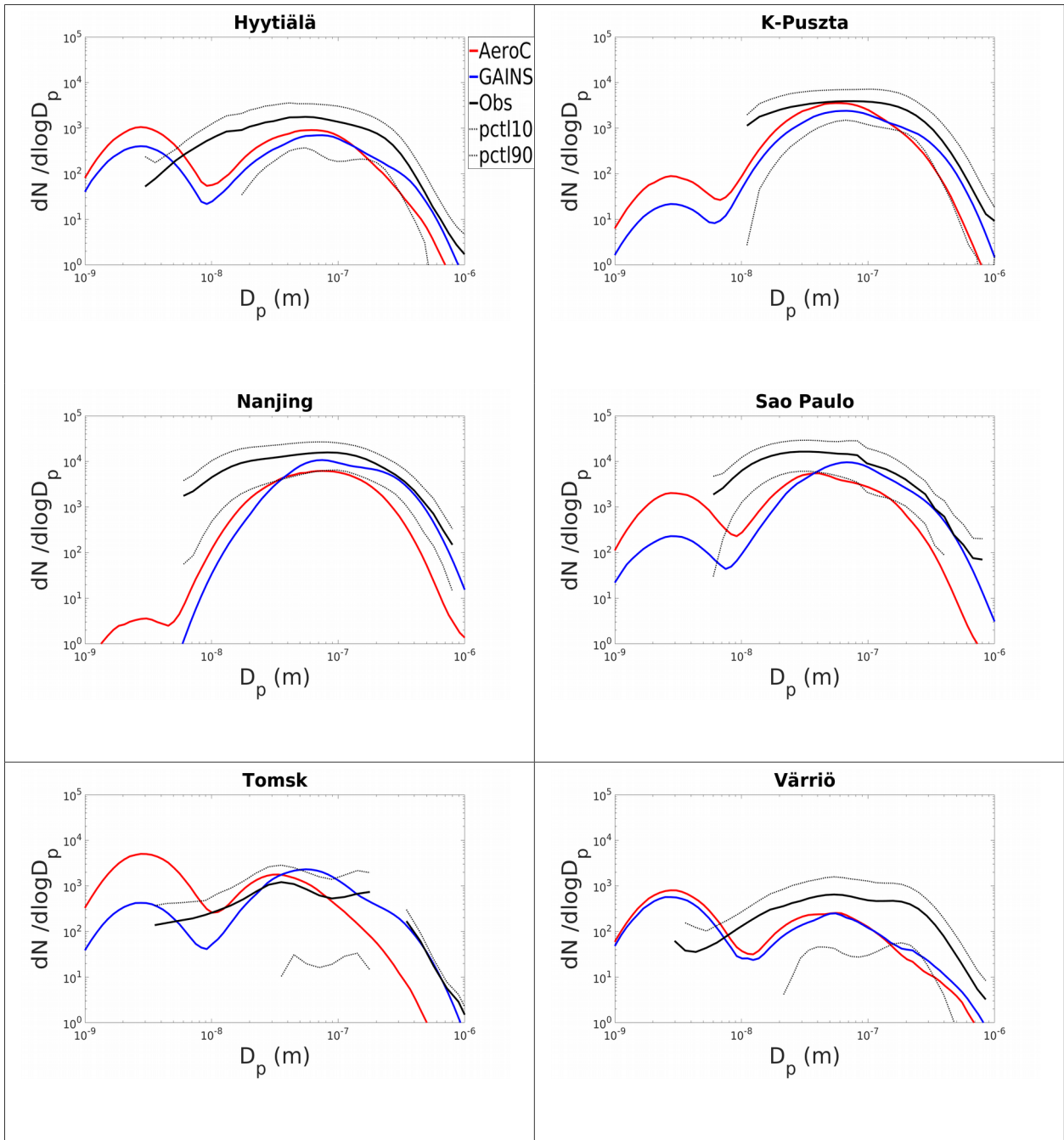
1142



1143 Figure 3. Total absolute anthropogenic emissions for (a) AeroCom and (b) GAINS without
 1144 visual interpolation.

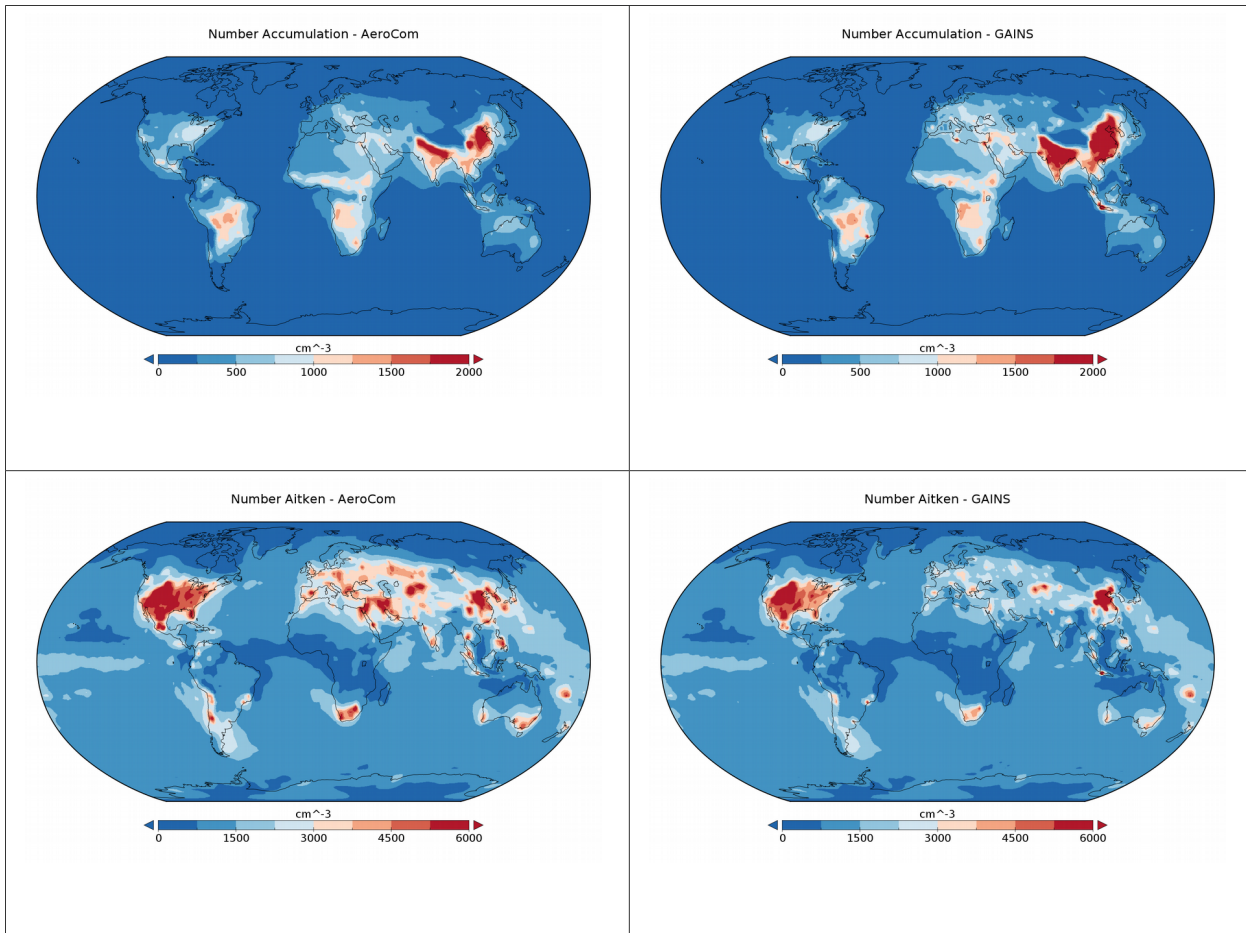


1145 Figure 4. Annual-averaged number of particles compared to observational data.
 1146 Measurement sites: 1: Botsalano; 2: Cabauw 3: Hohenpeissenberg; 4: Hyytiälä; 5: K-Pusztá;
 1147 6: Melpitz; 7: Nanjing; 8: Po Valley; 9: Sao Paulo; 10: Tomsk FNV; 11: Värriö. Both plots
 1148 include 1:1 and dashed 1:2, 2:1 lines.



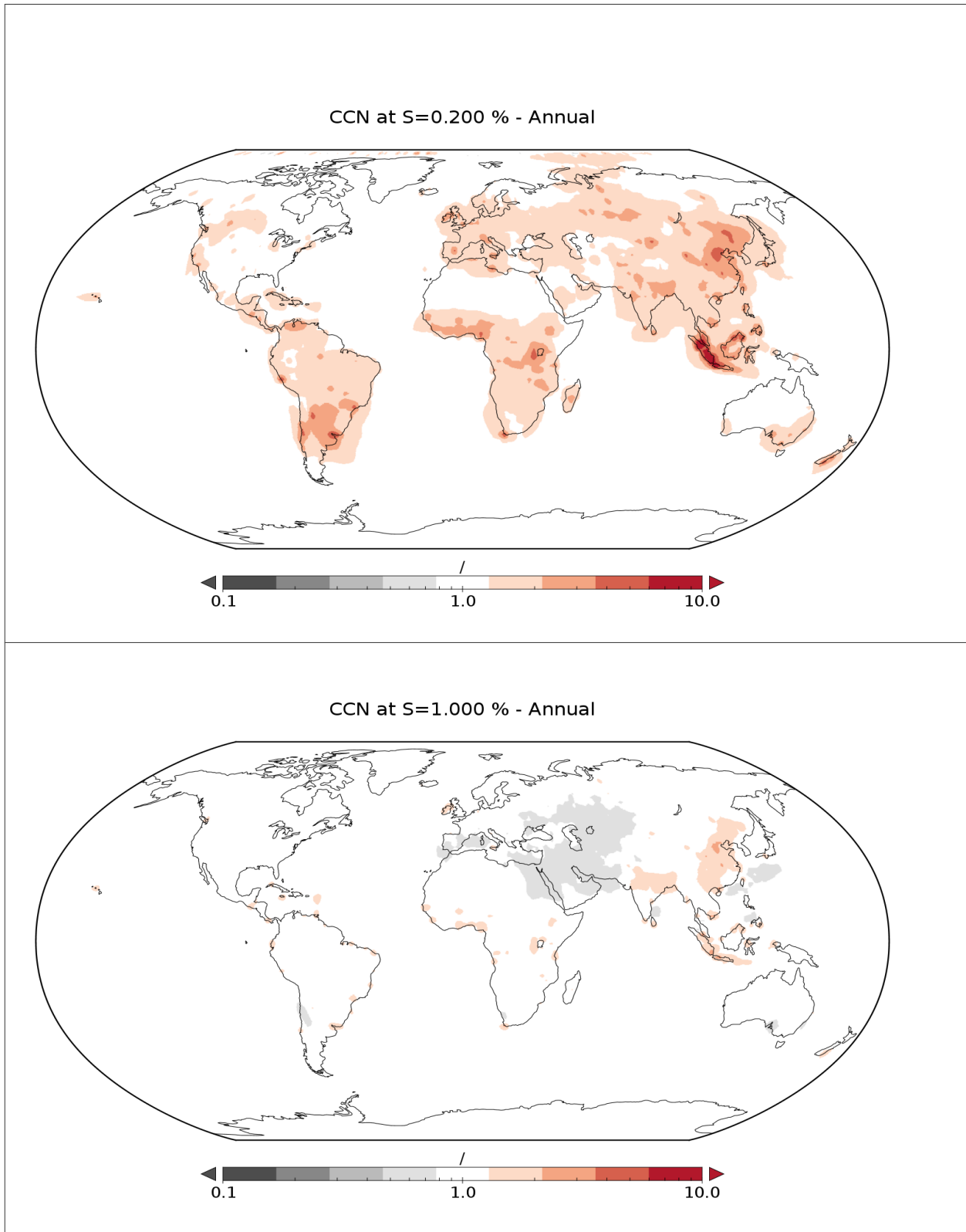
1149 Figure 5. Modeled particle number size distributions compared to observations at 6
 1150 measurement sites.

1151
 1152
 1153

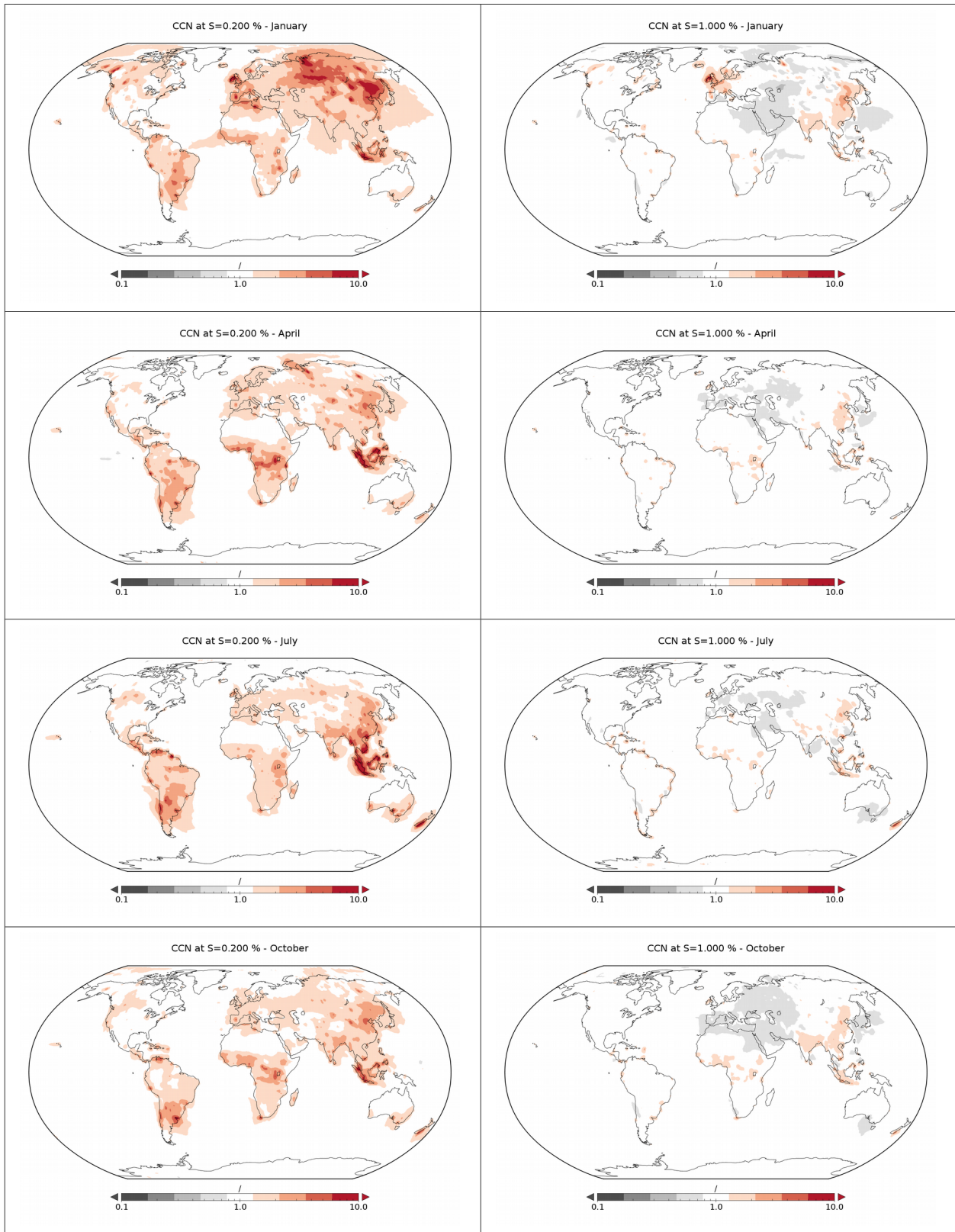


1154 Figure 6. Modeled annual particle number concentrations for accumulation mode (top) and
 1155 Aitken mode (bottom), at surface level.
 1156

1157
 1158
 1159
 1160
 1161
 1162
 1163
 1164
 1165
 1166
 1167
 1168
 1169
 1170
 1171
 1172
 1173
 1174



1175 Figure 7. Modeled annual GAINS/AeroCom ratios of CCN0.2 and CCN1.0, at surface level.



1176 Figure 8. Modeled seasonal GAINS/AeroCom ratios of CCN0.2 and CCN1.0, at surface level.